Plasma Electrodynamics and Applications

Academic and Research Staff
Professor Abraham Bers, Dr. Abhay K. Ram

Visiting Scientists and Research Affiliates
Prof. Alain Brizard (St. Michael's College, Colchester, Vermont), Dr. Yves Peysson (TORE-SUPRA, Commissariat à l'Énergie Atomique, Cadarache, France)

Graduate Students
Joan Decker, Brian C. Ross, David J. Strozzi

Technical and Support Staff
Laura M. von Bosau

Introduction

The work of this group is concerned with the electrodynamics of waves in plasmas, with phenomena relevant to controlled fusion energy generation in high-temperature plasmas that are confined magnetically or inertially, and with phenomena in space plasmas. We report on five studies of the past year.

On the electrodynamics of waves in plasmas, Section 1 reports on a multi-fluid hydrodynamic description of linear waves in a collisionless plasma confined in an external magnetic field $\vec{B}_0$ – a general description which is correct to first-order in finite-Larmor-radius (FLR) effects and for arbitrary frequency regimes. Section 2 shows how this is applied to understand the dispersion relation transformation of a cold-plasma extraordinary (X) wave to a kinetic electron-Bernstein wave (EBW) as the wavelength (perpendicular to $\vec{B}_0$) decreases in the regime of the upper-hybrid resonance frequency. This regime is of importance to coupling external power to EBWs in high-β, spherical tokamaks for current drive in such plasmas.

Sections 3 and 4 describe our accomplishments in studies of plasma heating and current drive in magnetically confined fusion plasmas. Section 3, in particular, describes the analysis and computational results on new means for generation of plasma current with EBWs that are driven by external RF (mm-wave) power sources. Section 4 describes the achievement and implementation of a general purpose computer code (DKE) for calculating plasma heating and current drive in tokamak confined plasmas. This code was used to obtain the results described in Section 3.

Section 5 describes the development of a one-dimensional, collisionless kinetic code (ELVIS) for studying the nonlinear evolution of intense laser-plasma interactions of interest to inertial fusion.

1. Hydrodynamics of Collisionless Waves in a Magnetic Field

Sponsors
Department of Energy (DoE) Contract DE-FG02-91ER-54109

Project Staff
Professor A. Bers

A multi-fluid hydrodynamic description of linear dynamics in a cold-plasma model[1,2] (i.e., when thermal effects are ignored) exhibits singularities in the natural waves propagating across an externally applied magnetic field $\vec{B}_0$. At these singularities – so-called resonances in propagation – their wavelengths $(\lambda_\perp = 2\pi / k_\perp)$ vanish, thus violating the fundamental, local requirement of a hydrodynamic description – namely, that the wavelength perpendicular to $\vec{B}_0$ be large compared to the average (thermal) particle's cyclotron radius $(\rho_T = \upsilon_T / \omega_c)$; i.e., that so-called finite-Larmor-radius (FLR) effects $(k_\perp \rho_T)$ be negligible. One way to remedy this situation (without going to a much more complex, kinetic plasma description) is to construct a hydrodynamic description in which FLR effects are accounted for to lowest order (in $k_\perp^2 \rho_T^2 < 1$).

Attempts to construct such a hydrodynamic description for a plasma go back to the early days of modern (high-temperature) plasma physics development, when interest was focused on the description of collisional transport phenomena in plasmas confined by a strong, external magnetic field, and on the single-fluid magneto-hydrodynamic (MHD) description of low-frequency dynamics.[3,4] For a plasma in a strong magnetic field, so-called gyro-viscous terms, that are independent of collisions, were discovered and their use became a common feature in collisionless MHD. Here we report on a different formulation of collisionless hydrodynamics for a plasma in a magnetic field, relevant to high frequency wave propagation in plasmas. In this regime, the simplest approach of including thermal effects is by adding an isotropic thermal pressure force to the cold-plasma momentum equation for each species of charged particles in the plasma, and (for closure of the equations) relating the isotropic thermal pressure to the plasma density through an ad-hoc equation of state.[1] Satisfactory results are sometimes obtained from this simple model by appropriately choosing (*a posteriori*) the free parameter in the equation of state. However, fundamentally, this approach suffers from the constraint that perturbations in pressure are isotropic, which is particularly restrictive, and generally unjustified, for dynamics in a magnetic field. Instead, in addition to the collisionless continuity and momentum equations, we use the collisionless dynamic equation for the anisotropic pressure, and close this set of hydrodynamic equations by assuming that, in the space-time scales of interest, heat flow can be neglected. This set of collisionless hydrodynamic equations, when solved to first-order in $(k_\perp \rho_T)^2$, is shown to lead to the identical linear plasma susceptibility tensor as derived from the Vlasov equation when the Vlasov susceptibility tensor is expanded to first-order in $(k_\perp \rho_T)^2$ and $(1/\zeta_n^2) = [k_\parallel \upsilon_T /(\omega - n\omega_c)]^2$, retaining only terms with $n = 0, \pm 1$, and ± 2, and ignoring (exponentially small) Landau and Doppler-shifted cyclotron dissipation terms.[1]

---

[1] W. P. Allis, S. J. Buchsbaum, and A. Bers, *Waves in Anisotropic Plasmas* (Cambridge, Massachusetts: M.I.T. Press), 1963; also (Tokyo, Japan: University of Tokyo Press, International Edition), 1964. (An errata for this book is available from A. Bers, upon request.)
[2] T. H. Stix, *Waves in Plasmas,* (New York: American Institute of Physics), 1992.
[3] W. B. Thompson, "The Dynamics of High Temperature Plasmas," *Reports on Progress in Physics* 24(1): 363–424 (1961).
[4] S. I. Braginskii, "Transport Processes in a Plasma," in *Reviews of Plasma Physics,* Vol. 1, ed. M. A. Leontovich (New York: Consultants Bureau), 1965, pp. 205–311.

Starting with the non-relativistic, collisionless Boltzmann equation, also known as the non-relativistic Vlasov equation, for the one-particle distribution function $f(\underline{w},\underline{r},t)$ of any charged particle species in the plasma, and taking the first three moments [w^o, $m\underline{w}$, and $m\underline{u}\underline{u}$, where $\underline{u}=\underline{w}-\underline{v}$ and $\underline{v}\equiv\underline{v}(\underline{r},t)$ is the average velocity over f] of the Vlasov equation, one obtains[5]

$$\frac{\partial n}{\partial t}+\nabla\cdot(n\underline{v})=0 \tag{1}$$

$$mn\left(\frac{\partial}{\partial t}+\underline{v}\cdot\nabla\right)\underline{v}+\nabla\cdot\overline{\overline{P}}=qn(\underline{E}+\underline{v}\times\underline{B}) \tag{2}$$

$$\left(\frac{\partial}{\partial t}+\underline{v}\cdot\nabla\right)\overline{\overline{P}}+(\nabla\cdot\underline{v})\overline{\overline{P}}+\left[\left(\overline{\overline{P}}\cdot\nabla\underline{v}\right)+(t)\right]+\nabla\cdot\overline{\overline{\overline{Q}}}=-\frac{q}{m}\left[\left(\underline{B}\times\overline{\overline{P}}\right)+(t)\right] \tag{3}$$

where (t) stands for the transpose of the preceding term inside the brackets. In these hydrodynamic equations, n is the average particle density,

$$\int f d^3w=n(\underline{r},t), \tag{4}$$

$\underline{v}$ is the average particle velocity,

$$\langle\underline{w}\rangle=\frac{1}{n}\int\underline{w}f d^3w\equiv\underline{v}(\underline{r},t), \tag{5}$$

$\overline{\overline{P}}$ is the thermal pressure tensor,

$$nm\langle\underline{u}\underline{u}\rangle=\int m\underline{u}\underline{u}f d^3w\equiv\overline{\overline{P}}, \tag{6}$$

and $\overline{\overline{\overline{Q}}}$ is the heat flow tensor,

$$\overline{\overline{\overline{Q}}}=nm\langle\underline{u}\underline{u}\underline{u}\rangle=m\int\underline{u}\underline{u}\underline{u}f d^3w. \tag{7}$$

As stated above, for our purposes, we close this set of hydrodynamic equations by setting $\nabla\cdot\overline{\overline{\overline{Q}}}=0$.

Next, we consider a drift-free ($\underline{v}_0=0=\underline{E}_0$), spatially homogeneous, and time-independent equilibrium, in an externally applied magnetic field $\underline{B}_0=\hat{b}B_0$, for which one can readily show from (**Error! Reference source not found.**–(3) that the equilibrium pressure must be of the form

$$\overline{\overline{P}}_0=P_{0\perp}\overline{\overline{I}}+(P_{0\|}-P_{0\perp})\hat{b}\hat{b} \tag{8}$$

with $P_{0\|}$ and $P_{0\perp}$ the equilibrium pressures, respectively, parallel and perpendicular to $\underline{B}_0$. For a thermal equilibrium, which we assume henceforth, $P_{0\|}=P_{0\perp}$ and

$$\overline{\overline{P}}_0=n_0\kappa T\overline{\overline{I}} \tag{9}$$

where $\overline{\overline{I}}$ is the unit-diagonal, second-rank tensor.

[5] J.-L. Delcroix and A. Bers, *Physique des Plasmas,* Vol. 2 (Paris, France: InterÉditions/CNRS Éditions), 1994, Chapter 9 and references therein. (An errata for both volumes is available from A. Bers, upon request.)

Linearizing the closed set of hydrodynamic equations [(**Error! Reference source not found.**–(3) with $\nabla \cdot \overline{\overline{Q}} = 0$] about the general equilibrium (8), we obtain

$$\frac{\partial n_1}{\partial t} + n_0 \nabla \cdot \vec{v}_1 = 0 \tag{10}$$

$$m n_0 \frac{\partial \vec{v}_1}{\partial t} + \nabla \cdot \overline{\overline{P}}_1 = q n_0 (\vec{E}_1 + \vec{v}_1 \times \vec{B}_0) \tag{11}$$

$$\frac{\partial \overline{\overline{P}}_1}{\partial t} + (\nabla \cdot \vec{v}_1)\overline{\overline{P}}_0 + \left[\left(\overline{\overline{P}}_0 \cdot \nabla \vec{v}_1\right) + (t)\right] = -\frac{q}{m}\left[\left(\vec{B}_0 \times \overline{\overline{P}}_1 + \vec{B}_1 \times \overline{\overline{P}}_0\right) + (t)\right] \tag{12}$$

where the subscript 1 denotes the small-amplitude fields. Using Faraday's equation to replace $\vec{B}_1$ by $\vec{E}_1$, and using Fourier-Laplace transforms we can solve for $\overline{\overline{P}}_1$ from the transform of (12) and substitute it into the transform of (11) to find the first-order current density $\vec{J}_1 = q n_1 \vec{v}_1$ (for the particular particle species) as a function of $\vec{E}_1$, and thus

$$\vec{J}_1(\vec{E}_1) \equiv -i\omega\, \varepsilon_0 \overline{\overline{\chi}} \cdot \vec{E}_1 \tag{13}$$

which defines the linear susceptibility tensor $\overline{\overline{\chi}} \equiv \overline{\overline{\chi}}(\vec{k}, \omega)$. When summed over species, (13) gives the total linear current density, which enters into the transformed Maxwell equations for the self-consistent fields. In the absence of external excitations, the latter equations then lead to the dispersion relation for the natural wave-modes of the plasma. We shall not give here this long and algebraically tedious calculation, but only summarize the result for the linear susceptibility of a thermal equilibrium (9) plasma, evaluated to first order in small parameters

$$\left(\frac{k_\parallel v_T}{\omega}\right)^2 << 1; \quad (k_\perp \rho_T)^2 << 1; \quad \left(\frac{k_\parallel v_T}{\omega}\right)(k_\perp \rho_T) << 1 \tag{14}$$

as is required for the validity of a collisionless hydrodynamic description. One thus finds

$$\overline{\overline{\chi}} \approx \overline{\overline{\chi}}_C + \delta^2 \overline{\overline{\chi}}_T \tag{15}$$

where $\delta^2 = (v_T / c)^2$, and, for simplicity, writing out $\overline{\overline{\chi}}$ for electrons only: $\overline{\overline{\chi}}_C$ is the cold plasma linear susceptibility

$$\overline{\overline{\chi}}_C = \begin{bmatrix} \chi_\perp & -i\chi_\times & 0 \\ i\chi_\times & \chi_\perp & 0 \\ 0 & 0 & \chi_\parallel \end{bmatrix} \tag{16}$$

$$\chi^C_{xx} = \chi^C_{yy} = \chi_\perp = \frac{-\alpha^2}{1-\beta^2}, \quad \alpha = \frac{\omega_{pe}}{\omega} \tag{17}$$

$$\chi^C_{xy} = -i\chi_\times = i\beta \frac{\alpha^2}{1-\beta^2}, \quad \beta = \frac{\omega_{ce}}{\omega} > 0 \tag{18}$$

$$\chi^C_{zz} = \chi_\parallel = -\alpha^2 \tag{19}$$

and the elements of $\overline{\overline{\chi}}_T$ are:

$$\chi_{xx}^{T} = \chi_{\perp}\left[\frac{1+3\beta^2}{(1-\beta^2)^2}\, n_{\parallel}^2 + \frac{3n_{\perp}^2}{(1-4\beta^2)}\right] \tag{20}$$

$$\chi_{yy}^{T} = \chi_{\perp}\left[\frac{1+3\beta^2}{(1-\beta^2)^2}\, n_{\parallel}^2 + \frac{1+8\beta^2}{(1-4\beta^2)} n_{\perp}^2\right] \tag{21}$$

$$\chi_{zz}^{T} = \chi_{\parallel}\left[3n_{\parallel}^2 + \frac{n_{\perp}^2}{(1-\beta^2)}\right] \tag{22}$$

$$\chi_{xy}^{T} = -i\chi_{\times}\left[\frac{3+\beta^2}{(1-\beta^2)^2} n_{\parallel}^2 + \frac{6n_{\perp}^2}{(1-4\beta^2)}\right] = -\chi_{yx}^{T} \tag{23}$$

$$\chi_{xz}^{T} = \chi_{\perp}\frac{2n_{\parallel} n_{\perp}}{(1-\beta^2)} = \chi_{zx}^{T} \tag{24}$$

$$\chi_{yz}^{T} = i\chi_{\times}\left(\frac{3-\beta^2}{1-\beta^2}\right) n_{\parallel} n_{\perp} = -\chi_{zy}^{T} \tag{25}$$

The results in (15)–(25) are found to be identical to those found from a low-temperature (or strong magnetic field) expansion of the linear susceptibility of a Maxwellian plasma derived from the Vlasov equation,[1] i.e., expanded to lowest order in the small parameters $(k_{\perp}\rho_T)^2$ and $(1/\zeta_n^2)$, and retaining only terms $n = 0, \pm 1$, and ± 2.[6] [See equations under (6.16) on page 90 of reference 1, and note a minor misprint/omission: the K_{xy} term should have a $1+$ inserted inside, at the beginning of the large parenthesis.] Note, of course, that the hydrodynamic results for non-zero $(1/\zeta_n^2) << 1$ will not show the exponentially small Landau and Doppler-shifted cyclotron dissipation terms that exist in $\overline{\overline{\chi}}_T$ derived from the Vlasov expansion.

Finally, the linear natural modes in this collisionless hydrodynamic description are obtained by using the derived linear susceptibility (15) in the dispersion relation,

$$D(\underline{k}, \omega) = \det[\overline{\overline{D}}(\underline{k}, \omega)] = 0 \tag{26}$$

where

$$\overline{\overline{D}}(\underline{k}, \omega) = \underline{\hat{n}}\,\underline{\hat{n}} - n^2 \overline{\overline{I}} + \overline{\overline{K}}(\underline{k}, \omega) \tag{27}$$

with $\underline{\hat{n}} = (c\underline{k}/\omega)$ and $\overline{\overline{K}} = \overline{\overline{I}} + \overline{\overline{\chi}}$. A particular application of these results is given in the next section.

[6] A. G. Sitenko and K. N. Stepanov, "On the Oscillations of an Electron Plasma in a Magnetic Field," *Soviet Physics–JETP* 4(4): 512–520 (1957).

2. Transformation of the Electromagnetic SX Mode to an Electrostatic Electron Bernstein Wave (EBW)

Sponsors
Department of Energy (DoE) /National Spherical Tokamak Experiment (NSTX) Contract DE-FG02-99ER-54521

Project Staff
Professor A. Bers and J. Decker

We have applied the analysis presented in Section 1 to obtain further understanding of mode conversion excitation of EBWs for heating and current drive in ST-type plasmas, e.g., the National Spherical Tokamak Experiment (NSTX) at the Princeton Plasma Physics Laboratory in New Jersey and the Mega-Amp Spherical Tokamak (MAST) at the Culham Science Centre in the U.K. As we have shown in the past,[7,8,9] in either mode-conversion scenario of X-B or O-X-B, the dispersion characteristics of the natural modes, in the vicinity of the upper-hybrid frequency $[\omega_{UH} = (\omega_p^2 + \omega_{ce}^2)^{1/2}]$, undergo a transformation from an electromagnetic cold-plasma SX mode (at small $k_\perp$) to an electrostatic, kinetic EBW (at large $k_\perp$). To properly describe this transformation, when ω_{UH} is in the vicinity of ω_{ce} or $2\omega_{ce}$, it requires that thermal effects be properly accounted for to order $(k_\perp \rho_T)^2$. In the absence of thermal effects (i.e., in a cold plasma) the SX-mode dispersion near ω_{UH} becomes singular $(k_\perp \to \infty)$ – a nonphysical result of the cold plasma model. Accounting for thermal effects by a hydrodynamic description in which the pressure perturbations are isotropic leads to (incorrect) results that show the transformation to a kinetic mode occurs at $(k_\perp \rho_T) >> 1$, which in itself violates the hydrodynamic model assumptions. Allowing for the perturbations in pressure to be anisotropic, as in Section 1, shows that the transformation occurs for $(k_\perp \rho_T)^2 < 1$, consistent with the validity of hydrodynamics presented in Section 1. Here, for simplicity, we illustrate this for propagation perpendicular to $\underset{\sim}{B}_0$, i.e., we take $k_\parallel = 0$.

From the analytical results of Section 1, the hydrodynamic description allowing for arbitrary anisotropic thermal pressure perturbations leads to the dispersion relation correct to order $(k_\perp \rho_T)^2$ which is of the form:

$$\delta^2 b_{xx} n_\perp^6 + (A_\perp + \delta^2 A_{Th}) n_\perp^4 + (B_\perp + \delta^2 B_{Th}) n_\perp^2 + (C_\perp + \delta^2 C_{Th}) = 0 \qquad (28)$$

For $\delta^2 = (\upsilon_T / c)^2 = 0$, one readily recovers from (28) the well-known cold-plasma dispersion relation.[1,2] In general, the thermal correction coefficients multiplied by δ^2 in this equation for $n_\perp^2 = (ck_\perp / \omega)^2$ depend upon $n_\parallel^2 = (ck_\parallel / \omega)^2$. For the simple case of $k_\parallel = 0 = n_\parallel$, $C_{Th} = 0$ (showing that the cutoffs, i.e., $n_\perp = 0$, are the same as in a cold plasma) and the other thermal correction coefficients simplify considerably. Furthermore, in the vicinity of $\omega \approx \omega_{UH}$ where $n_\perp^2$ becomes large (infinite in the case of a cold plasma at $\omega = \omega_{UH}$), the dispersion relation can be even further simplified by ignoring $C_\perp$, B_{Th}, and

[7] A. Bers, A. K. Ram, and S. D. Schultz, "Coupling to Electron Bernstein Waves in Tokamaks," *Proc. 2nd Europhysics Topical Conference on RF Heating and Current Drive of Fusion Devices,* Brussels, Belgium, January 20–23, 1998, Contributed Papers, European Physical Society, Vol. 22A (eds. J. Jacquinot, G. Van Oost, and R. R. Weynants), Petit-Lancy, Switzerland (1998), pp. 237–240.
[8] A. K. Ram and S. D. Schultz, "Excitation, Propagation, and Damping of Electron Bernstein Waves in Tokamaks," *Phys. Plasmas* 7(10): 4084–4094 (2000).
[9] A. K. Ram, A. Bers, and C. N. Lashmore-Davies, "Emission of Electron Bernstein Waves in Plasmas," *Phys. Plasmas* 9(2): 409–18 (2002).

A_{Th} , and obtaining the reduced dispersion relation

$$\delta^2 A_{TR} n_\perp^4 + A_{CR} n_\perp^2 - B_{CR} \approx 0 \tag{29}$$

where

$$A_{TR} \approx \frac{-3\omega_{UH}^2}{\omega_{UH}^2 - (2\omega_{ce}^2)^2} \tag{30}$$

$$A_{CR} \approx \frac{2\omega_{UH}}{\omega_p^2}(\omega - \omega_{UH}) \tag{31}$$

$$B_{CR} \approx -\frac{\omega_{ce}^2}{\omega_{UH}^2} \tag{32}$$

The subscript R indicates that the coefficients $(b_{xx})_R \equiv A_{TR}$, $(A_\perp)_R \equiv A_{CR}$, and $(B_\perp)_R \equiv -B_{CR}$, have been evaluated in the vicinity of $\omega^2 \approx \omega_{UH}^2$. It is readily evident from the sign of A_{TR} in (30) that the solution of this quadratic equation in $n_\perp^2$ is different for when $\omega_{UH} < 2\omega_{ce}$, and for $\omega_{UH} \tilde{>} 2\omega_{ce}$. The behavior of the dispersion relation in the vicinity of ω_{UH} for these two cases is illustrated in Figure 1(a) and (b).

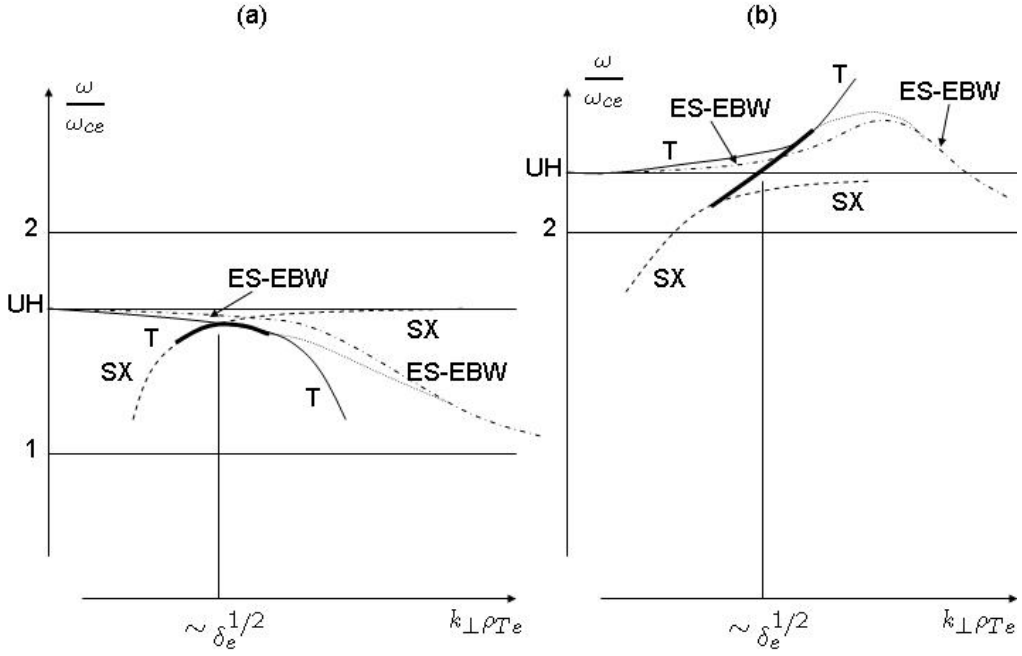

Figure 1: Sketch of the dispersion relation (ω/ω_{ce}) vs $(k_\perp \rho_{Te})$ near $\omega = \omega_{UH}$, for (a) $\omega_{UH} < 2\omega_{ce}$ and (b) $\omega_{UH} > 2\omega_{ce}$. Only propagating solutions (real ω and real $k_\perp$) are shown. Dashed curves show the uncoupled SX and thermal T modes; solid T curves are the coupled mode solutions; dot-dashed curves are the electrostatic electron Bernstein waves (ES-EBW); dotted curves show the (presumed) connection of the solid T curves to the ES-EBW at large $k_\perp \rho_{Te}$.

Note from Figure 1(a) that for $\omega_{UH} < 2\omega_{ce}$, as $(k_\perp \rho_{Te})$ increases from small values, the forward ($v_p v_g > 0$, where v_p is the phase velocity and v_g is the group velocity) electromagnetic SX mode (shown in dashed lines), before reaching ω_{UH}, transforms to a backward ($v_p v_g < 0$) "thermal mode" (shown in solid line), and thus never reaches $\omega = \omega_{UH}$. As can be easily shown from (29), this transformation occurs for small (but non-zero) $(k_\perp \rho_{Te})$ proportional to $\delta_e^{1/2} << 1$, and thus the thermal mode description is valid within the used hydrodynamic model of Section 1. As $(k_\perp \rho_{Te})$ increases further, the hydrodynamic thermal mode ceases to be valid, and the mode changes (shown in dotted line) to the kinetic, electrostatic EBW mode for $\omega_{UH} < 2\omega_{ce}$ (shown in dot-dashed line). Note also that the kinetic, electrostatic EBW which for $k_\perp = 0$ goes to $\omega = \omega_{UH}$ is invalid for $(k_\perp \rho_{Te})$ below the thermal mode, since then the mode becomes electromagnetic (the SX mode) and the electrostatic approximation for the EBW no longer holds.

On the other hand, note from Figure 1(b) that for $\omega_{UH} > 2\omega_{ce}$, as $(k_\perp \rho_{Te})$ increases from small values, the forward, electromagnetic SX mode (shown in dashed lines) becomes a forward "thermal mode" (shown in solid line) that crosses $\omega = \omega_{UH}$,[10] and as $(k_\perp \rho_{Te})$ increases further the thermal mode changes (shown in dotted line) to become the kinetic, electrostatic EBW mode for $2\omega_{ce} < \omega < 3\omega_{ce}$. Here as well, the kinetic electrostatic EBW, which for $k_\perp \to 0$ approaches $\omega \to \omega_{UH}$, is invalid for $(k_\perp \rho_{Te})$ below the thermal mode.

The different behavior of the dispersion relation near $\omega = \omega_{UH}$, for $\omega_{UH} < 2\omega_{ce}$ and $\omega_{UH} > 2\omega_{ce}$ has been pointed out before from specific numerical solutions of the full electromagnetic, kinetic dispersion relation based upon the linearized Vlasov-Maxwell equations,[11] but not explained. An analysis similar to ours can be found in[12]. The advantage of showing that the dispersion transition can be based upon a proper hydrodynamic description is that such a description is more readily amenable to a detailed mode-conversion analysis for an inhomogeneous plasma[7,8,9] than a kinetic description would be.

Finally, we remark that our hydrodynamic analysis can be readily extended to include non-zero $k_\parallel$, as long as these are sufficiently small so that Landau and Doppler-shifted cyclotron damping are negligible (see Section 1).

---

[10] It should be noted that at $\omega = \omega_{UH}$, $(A_T)_R \equiv A_{CR} = 0$ so that neglecting $(\delta^2 A_{Th})$ in (28) is not justified. However, for $\delta^2 << 1$, accounting for $(\delta^2 A_{Th})$ in (29) leads to only a small shift in the dispersion at $\omega = \omega_{UH}$.

[11] S. Puri, F. Leuterer, and M. Tutter, "Dispersion Curves for the Generalized Bernstein Modes," *J. Plasma Phys.* 9(1): 89–100 (1973).

[12] A. I. Akhiezer, I. A. Akhiezer, R. V. Polovin, A. G. Sitenko, and K. N. Stepanov, *Plasma Electrodynamics, Vol. 1: Linear Theory* (Oxford, New York: Pergamon Press), 1975.

3. Ohkawa Current Drive by Electron Bernstein Waves in Spherical Tori

Sponsors
Department of Energy (DoE) Contract DE-FG-91ER-54109 and Department of Energy (DoE) /National Spherical Tokamak Experiment (NSTX) Contract DE-FG02-99ER-54521

Project Staff
J. Decker, Dr. A. K. Ram, Professor A. Bers, and Dr. Y. Peysson

Spherical Tori (ST) are tight aspect ratio tokamaks ($R_0 / a \sim 1.5$ in NSTX, where R_0 is the major radius and a is the minor radius) that are attractive because of their ability to achieve high-β regimes ($\beta = 2\mu_0 \langle p \rangle / B_0^2$, where $\langle p \rangle$ is the volume averaged pressure and B_0 the plasma toroidal field on axis). Since ST are very overdense ($\omega_c << \omega_p$, where ω_c is the cyclotron frequency and ω_p is the plasma frequency), current drive (CD) using electron cyclotron (EC) waves is difficult and inefficient. However, it has been shown that, in the EC range of frequencies, it is possible to externally excite electron Bernstein waves (EBW) by mode conversion (MC) at the edge of ST plasma.[7] In addition, EBW can propagate in the plasma without density limits and are strongly damped at any harmonic of the EC resonance.[8] Current drive by EBW has been recently demonstrated in toroidally confined fusion plasmas.[13,14] As EBW received much consideration for CD in ST experiments such as NSTX, MAST and CDX-U, it is important to describe the process of EBWCD in order to design and optimize these experiments. Using our kinetic code DKE,[15,16,17] we are solving the kinetic equation with Fokker-Planck (FP) collisions and quasilinear (QL) diffusion due to EBW. In addition, we account for the effects of magnetic trapping of electrons, which are important in ST. We show that large current densities can be driven in high-β regimes of ST, and that this current is primarily driven by the Ohkawa[18,19,20] mechanism, which shows the central role of magnetic trapping of electrons in the ST physics.

---

[13] V. Shevchenko, Y. Baranov, M. O'Brien, and A. Saveliev, "Generation of Noninductive Current by Electron-Bernstein Waves on the COMPASS-D Tokamak," *Phys. Rev. Lett.* 89(26): 265005/1–4 (2002).
[14] H. P. Laqua, H. Maassberg, N. B. Marushchenko, F. Volpe, A. Weller, and W. Kasparek, "Electron-Bernstein-Wave Current Drive in an Overdense Plasma at the Wendelstein 7-AS Stellarator," *Phys. Rev. Lett.* 90(7): 075003/1–4 (2003).
[15] J. Decker, Y. Peysson, A. Bers, and A. K. Ram, "Plasma Electrodynamics and Applications: Section 3 – New Code and Results on LHCD and ECCD Synergism With the Bootstrap Current," *Progress Report No. 144,* MIT Research Laboratory of Electronics, Cambridge, 2002, Chapter 16, pp. 23–27 http://rleweb.mit.edu/Publications/pr144/default.htm.
[16] J. Decker, Y. Peysson, A. Bers, and A. K. Ram, "Plasma Electrodynamics and Applications: Section 2 – Self-Consistent Calculation of ECCD and OKCD With the Bootstrap Current," *Progress Report No. 145,* MIT Research Laboratory of Electronics, Cambridge, 2003, pp. 16-7 – 16-11 http://rleweb.mit.edu/pr2002/files/pdfs/16.pdf.
[17] J. Decker, Y. Peysson, A. Bers, and A. K. Ram, "Plasma Electrodynamics and Applications: Section 4 – Numerical Code for Solving the Drift-Kinetic Equation in Tokamaks with Non-Circular Flux-Surfaces," *Progress Report No. 146,* MIT Research Laboratory of Electronics, Cambridge, 2004.
[18] T. Ohkawa, "Steady State Operation of Tokamaks by RF Heating," *General Atomics Company Report No.* GA-A13847 (1976).
[19] J. Decker, A. Bers, A. K. Ram, and Y. Peysson, "Plasma Electrodynamics and Applications: Section 1 – Ohkawa Versus Fisch-Boozer Method for Driving Current With Electron Cyclotron Waves," *Progress Report No. 145,* MIT Research Laboratory of Electronics, Cambridge, 2003, pp. 16-2 – 16-6 http://rleweb.mit.edu/pr2002/files/pdfs/16.pdf.
[20] J. Decker, "ECCD for Advanced Tokamak Operations Fisch-Boozer versus Ohkawa Methods," *Proc. 15th Topical Conference on Radio Frequency Power in Plasmas*, Moran, Wyoming, May 19–21, 2003, A.I.P. Conf. Proc. 694 (ed. C. B. Forest), Melville, New York (2003), pp. 447–454.

A. Modeling of CD by EBW

In this study, we do not investigate the problem of EBW excitation and propagation, which requires a modeling of the MC and also ray-tracing calculations. Instead, we concentrate on the EC resonance (ECR) region. Because of the strong, complete absorption of the EBW power at the Doppler-shifted ECR, the width of the radial power deposition profile is typically very narrow compared to the equilibrium scale lengths in the plasma. As a consequence, it is reasonable to assume the parallel index of refraction $n_{\|}$ to remain constant across the deposition region, where, in addition, the propagation path is assumed to be locally straight. Consequently, in our simulations, the EBW beam is modelized by a single, straight ray with a Gaussian parallel spectrum centered around a constant $k_{\|}$, and is assumed to be well focused, meaning that the poloidal extent of the beam satisfies $\Delta\theta_b << 2\pi$. The ray is then characterized by a parallel spectrum width $\Delta k_{\|} \approx 1/(r\Delta\theta_b)$. In addition, we assume a circular plasma.

Given the plasma equilibrium and the $k_{\|}$ spectrum of the wave, we calculate $k_{\perp}$ and the wave polarization and power flow by solving the wave equation, using our fully relativistic dispersion solver R2D2.[21]

We use these wave properties to evaluate the EBW QL diffusion coefficient and calculate the steady-state FP Equation with QL diffusion. The electron guiding-center drifts velocities across flux-surfaces are generally small compared to the streaming velocities along the field lines, and can be neglected in first approximation. In addition, for the equilibrium under consideration, we are in the low-collisionality (banana) regime in which the bounce time of trapped particles is much shorted than the collisional detrapping time. As a consequence, the distribution function is uniform along the field lines, and can be obtained by solving the 2D momentum space $(p_{\|}, p_{\perp})$ bounce-averaged FP equation

$$C(f) + Q(f) = 0 \tag{33}$$

where $C(f)$ is the collisions operator and $Q(f)$ is the EBW QL diffusion operator, which can be expressed as

$$Q(f) = \nabla_{\bar{p}} \cdot \overline{\overline{D}}^{RF} \cdot \nabla_{\bar{p}} f \tag{34}$$

with the following diffusion tensor elements

$$D_{\perp\perp}^{RF} = \sum_{n=-\infty}^{+\infty} \left[\frac{n\Omega}{\omega_b}\right]^2 D_{b,n}^{RF}(p_{\perp}, p_{\|}) \tag{35}$$

$$D_{\perp\|}^{RF} = \sum_{n=-\infty}^{+\infty} \frac{p_{\perp}}{p_{\|}} \frac{n\Omega}{\omega_b}\left[1 - \frac{n\Omega}{\omega_b}\right] D_{b,n}^{RF}(p_{\perp}, p_{\|}) \tag{36}$$

$$D_{\|\perp}^{RF} = \sum_{n=-\infty}^{+\infty} \frac{p_{\perp}}{p_{\|}} \frac{n\Omega}{\omega_b}\left[1 - \frac{n\Omega}{\omega_b}\right] D_{b,n}^{RF}(p_{\perp}, p_{\|}) \tag{37}$$

$$D_{\|\|}^{RF} = \sum_{n=-\infty}^{+\infty} \frac{p_{\perp}^2}{p_{\|}^2} \left[1 - \frac{n\Omega}{\omega_b}\right]^2 D_{b,n}^{RF}(p_{\perp}, p_{\|}) \tag{38}$$

[21] Y. Peysson, J. Decker, and R. W. Harvey, "Advanced 3-D Electron Fokker-Planck Transport Calculations," *Proc. 15th Topical Conference on Radio Frequency Power in Plasmas*, Moran, Wyoming, May 19–21, 2003, A.I.P. Conf. Proc. 694 (ed. C. B. Forest), Melville, New York (2003), pp. 495–498.

The QL diffusion tensors sums over all harmonics n, $\Omega = \omega_c / \gamma$ is the relativistic gyro-frequency, and ω_b is the EBW frequency. The QL diffusion coefficient $D_{b,n}^{RF}(p_\perp, p_\parallel)$ is given by the following expression

$$D_{b,n}^{RF} = D_{b,n,0}^{RF} \frac{\gamma p_{Te}}{|p_\parallel|} |\Theta_{b,n}|^2 \frac{1}{\sqrt{\pi}\Delta N_\parallel} e^{-(N_{\parallel \mathrm{res}} - N_{\parallel b})^2 / \Delta N_\parallel^2} \tag{39}$$

In (39), $D_{b,n,0}^{RF}$ is a constant with the dimension of a diffusion coefficient in momentum space, and can be normalized to the collisional diffusion coefficient as

$$\frac{D_{b,n,0}^{RF}}{v_e p_{Te}^2} = \frac{4\pi}{m_e \omega_{pe}^2 \ln\Lambda} \frac{\pi}{\omega_b} \frac{1}{|\bar{\Phi}_b \cdot \hat{n}_b|} \frac{P_{b,\mathrm{inc}}}{4\pi^2 r R_0} \tag{40}$$

It depends in particular on the incident wave power density $P_{b,\mathrm{inc}} / (4\pi^2 r R_0)$, and the power flow incidence factor $|\Phi_b \cdot n_b|$. The factor

$$\Theta_{b,n} = \frac{1}{\sqrt{2}} \varepsilon_b + J_{n-1}(z_b) + \frac{1}{\sqrt{2}} \varepsilon_b - J_{n+1}(z_b) + \frac{p_\parallel}{p_\perp} \varepsilon_{b,\parallel} J_n(z_b) \tag{41}$$

depends on the circular and parallel components of the electric field polarization vector ε and on Bessel functions J_n with argument $z_b = k_\perp \upsilon_\perp / \Omega$.

Finally, the resonance condition is found in the expression of $N_{\parallel \mathrm{res}}$

$$N_{\parallel \mathrm{res}} = \sqrt{\frac{m_e c^2}{Te}} \frac{p_{Te}}{p_\parallel} \left(\gamma - \frac{n\omega_{ce}}{\omega_b} \right) \tag{42}$$

B. Kinetic Calculations of Ohkawa EBWCD in NSTX

NSTX	
R_0 (m)	0.9
a (m)	0.6
B_0 (T)	0.35
I_0 (MA)	0.8
T_{e0} (keV)	3.0
n_{e0} (m^{-3})	3.0 x 10^{19}

Table 1: Equilibrium Properties in NSTX

In order to study EBWCD in a realistic ST scenario, we consider a typical NSTX plasma, with the equilibrium properties listed in Table 1. In this high-β regime, the poloidal magnetic field off-axis becomes comparable to the toroidal magnetic field, which creates a dip in the total magnetic field profile, as seen on Figure 2. This well is even more pronounced when we plot the Doppler-shifted second harmonic of the cyclotron frequency, as shown on Figure 3. We choose a frequency between the first and the second harmonic on the LFS, $\omega / 2\pi = 12$ GHz, which is shown as a red line on Figure 3. The value $N_\parallel = 1.5$ is chosen here because it is the one for which we find the largest driven current. It is interesting to note that the maximum CD is obtained for a value of $N_\parallel$ such that the EBW frequency is tangent to the profile of Doppler-shifted second harmonic cyclotron frequency. This result can be explained by the fact that in the present optimized case, the magnetic field profile is locally flat, meaning that the optical depth in very large. As a consequence, the power is deposited on energetic electrons far in the tail, which leads to larger CD efficiencies. The non-monotonic magnetic field profile has therefore important and positive implications on EBWCD in STs.

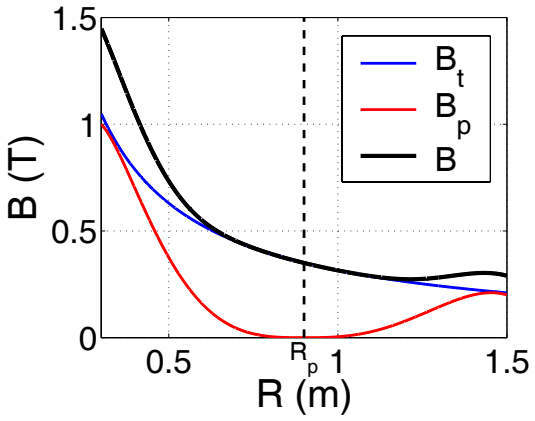

Figure 2: Toroidal (blue), poloidal (red) and total (black) magnetic field in NSTX.

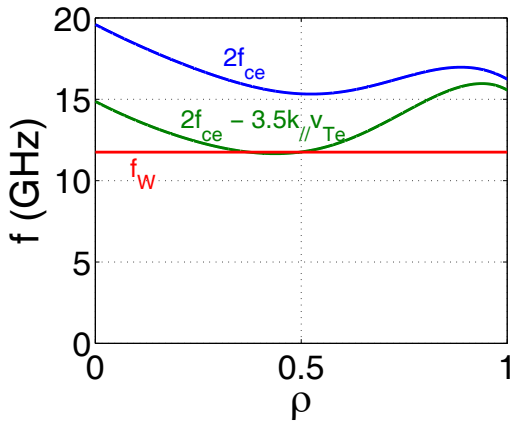

Figure 3: 2nd harmonic (blue) and Doppler-shifted (green) for $N_{\|} = 1.5$. EBW frequency in red.

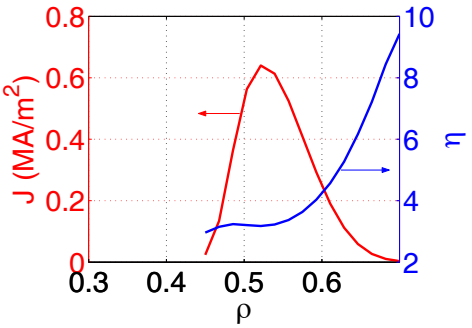

Figure 4: Driven current density (red) and figure of merit (blue).

The driven current density profile is shown on Figure 4. It is centered around the peak value $\rho_{\text{peak}} = 0.53$. We also show the figure of merit given by

$$\eta = \frac{J/(en_e v_{Te})}{P/(v_e m_e n_e v_{Te}^2)} \tag{43}$$

where J is the driven current density and P is the density of power absorbed. In this case, a total beam power of $P_{\text{inc}} = 1$ MW is absorbed, and a total current of $I = 87$ kA is driven.

In general, EBW are mostly electrostatic waves and therefore $N_{\perp} >> 1$. In the present case, we have $N_{\perp} = 12$ at $\rho = \rho_{\text{peak}}$. As a consequence, finite Larmor radius (FLR) effects are significant, and the factor $|\Theta_{b,n}|$ has several peaks in $p_{\perp}$ space. These peaks are apparent in the contour plot of the QL diffusion coefficient $D_{b,n}^{RF}$, shown as green lines in momentum space for $\rho = \rho_{\text{peak}}$ on Figure 5(a).

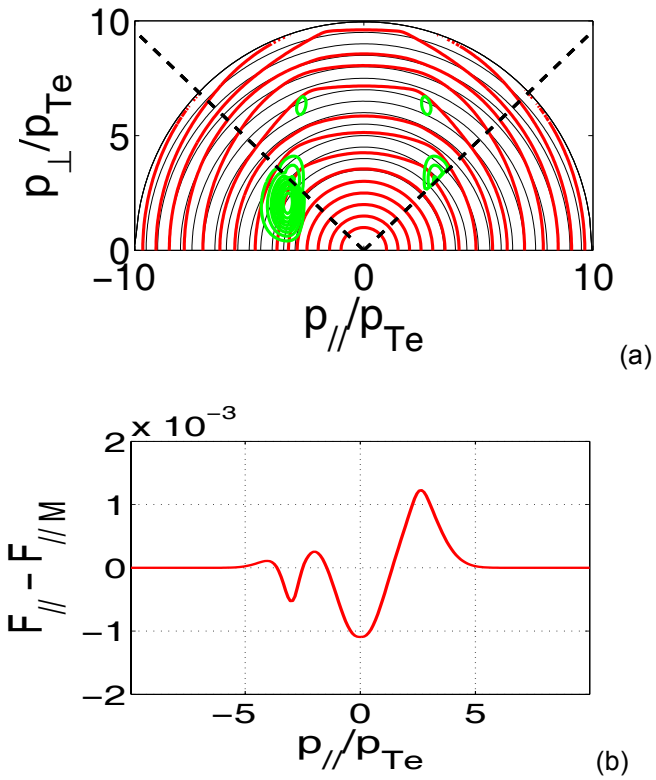

Figure 5: (a) Distribution function in EBWCD (red) and EBW QL diffusion coefficient (green). The unperturbed Maxwellian is in black. (b) Parallel distribution function.

On this figure are also plotted the unperturbed Maxwellian and the steady-state distribution function in EBWCD. The region of maximum diffusion is situated very near the trapped/passing boundary, and a large EBW-induced trapping takes place, since the diffusion is mostly in the perpendicular direction. As a consequence, a large Ohkawa current is driven. This current is more easily visualized on the "parallel" distribution function, obtained by integration over $p_\perp$ and plotted on Figure 5(b).

$$F_\parallel(p_\parallel) = 2\pi \int_0^\infty p_\perp dp_\perp f(p_\parallel, p_\perp) \tag{44}$$

The depletion of electron due to wave-induced trapping on the resonant side, and the accumulation of electrons due to detrapping on the opposite side, both contribute to driving a large Ohkawa current.

C. Conclusion

We have shown that a large Ohkawa EBW current could be driven off-axis $(\rho > 0.5)$ in ST plasmas. The Ohkawa effect is dominant because of

- the large fraction of trapped particles
- the dominantly perpendicular QL diffusion
- the large FLR effects which allow a positioning of the diffusion region right near the trapped/passing boundary in momentum space.

The large figure of merit is due to the very strong damping of the EBW, so that most of the power is deposited on very energetic, weakly collisional electrons. This effect can be enhanced, and the figure-of-merit improved, by locally flat magnetic field profiles in high-β ST. The resulting CD efficiency turns out to be several times larger than typical off-axis ECCD efficiencies in tokamaks.

4. Numerical Code for Solving the Drift-Kinetic Equation in Tokamaks with Non-circular Flux-Surfaces

Sponsors
Department of Energy (DoE) Contract DE-FG-91ER-54109 and Department of Energy (DoE) /National Spherical Tokamak Experiment (NSTX) Contract DE-FG02-99ER-54521

Project Staff
J. Decker, Dr. Y. Peysson, Professor A. Bers, and Dr. A. K. Ram

The calculation of current drive (CD) by radio-frequency (RF) waves in tokamaks requires one to solve the bounce-averaged drift-kinetic equation (DKE) with Fokker-Planck (FP) collisions and quasilinear (QL) diffusion due to the waves,[22] taking into account the effects of radial drifts and particle magnetic trapping. For the past three years, we have been involved, in collaboration with Yves Peysson from Cadarache, France, in the development of a fast, accurate DKE solver, which allowed us to calculate self-consistently RFCD and the bootstrap current (BC).[15,16] These simulations are of great interest for the development of advanced tokamak (AT) experiments, which rely primarily on these two sources of toroidal current to sustain the poloidal magnetic field.

However, until last year, our calculations were limited to the case of plasmas with circular, concentric flux-surfaces, which are not very realistic in modern tokamak experiments, where strong plasma shaping and high-β regimes lead to more complex flux-surface geometries. In addition, our models were limited to large aspect ratio toroidal plasmas and low-β scenarios for which the poloidal magnetic field was much smaller than the toroidal magnetic field.

In order to perform more realistic RFCD+BC calculations, in particular for the high-β, strongly shaped, low aspect ratio, so-called spherical tokamaks (ST), we have improved our description to account for arbitrary nested flux-surface geometry. More precisely, the bounce integrals, which account for the particle orbits along the field lines, are now performed numerically based on an arbitrary, given numerical equilibrium.

In Section A below, we give our description of the tokamak geometry, and calculate corresponding integral quantities such as the safety factor, the poloidal bounce or transit time, etc. We also define the bounce-averaging operation. In Section B, we present the DKE and describe the reduction of the equation in the small drift, low collisionality approximation. In Section C, we outline the principal features of our DKE solver. Finally, in Section D, we give the expression for the flux-surface averaged moments of the distribution function.

A. Particle Motion in Tokamaks

We consider a toroidal axisymmetric plasma immersed in a constant magnetic field, which can be expressed as

$$B = I(\psi)\nabla\phi + \nabla\psi\times\nabla\phi \tag{45}$$

where ψ is the poloidal flux and ϕ is the toroidal angle. $I(\psi)$ is a function related to the toroidal magnetic field. Its dependence upon ψ is a measure of the plasma diamagnetism. The field lines associated with the magnetic field B form closed, nested flux-surfaces, parametrized by the flux function ψ. If we define s as being the curvilinear length along the poloidal field lines, we obtain a local orthonormal coordinate system ($\underline{\psi}, \underline{s}, \underline{\phi}$) with $\underline{\psi} = \nabla\psi / |\nabla\psi|$, $\underline{s} = \nabla s$, and $\underline{\phi} = R\nabla\phi$, where R is the local toroidal major radius. We consider only electron motion, and assume in first approximation that

[22] C. F. F. Karney, "Fokker-Planck and Quasilinear Codes," *Comp. Phys. Rep.* 4(3-4), 183–244 (1986).

their orbit remains primarily on the same flux-surface (thin banana width approximation). Then, the poloidal transit or bounce time is given by

$$\tau_b(p,\psi) = \int_{s_{\min}}^{s_{\max}} \frac{ds}{|\upsilon_s|} \tag{46}$$

where $s_{\min}$ and $s_{\max}$ are such that the particle has performed one entire poloidal rotation between $s_{\min}$ and $s_{\max}$, if it is a passing particle, or they are the location of turning points, if it is a trapped particle. υ_s is the component of the velocity along the poloidal field lines. However, the (ψ, s, ϕ) coordinate system is not ideal for numerical integration. Instead, we use the system (ψ, θ, ϕ) where θ is the poloidal angle, taken with respect to the outboard horizontal mid-plane. We denote θ_0 the poloidal position, on the flux-surface, where the magnetic field magnitude is minimum: $B_0(\psi) = \min_\theta [B(\psi,\theta)]$. The subscript zero refers to quantities evaluated at $\theta = \theta_0$.

The guiding-center momentum space coordinate system is (p,ξ), where p is the momentum magnitude and $\xi = p_{\|}/p$ is the momentum projection along the field line. Using the conservation of energy and magnetic moment, p is a constant along the field line, while ξ varies according to

$$\xi(\psi,\theta,\xi_0) = \mathrm{sign}(\xi_0)\sqrt{1-\Psi(\psi,\theta)(1-\xi_0^2)} \tag{47}$$

where $\Psi(\psi,\theta)$ is the ratio of the magnetic field to its minimum on the flux-surface

$$\Psi(\psi,\theta) \equiv \frac{B(\psi,\theta)}{B_0(\psi)} \tag{48}$$

As a consequence, electrons, which are characterized by (ψ, p, ξ_0), are trapped if

$$\xi_0^2 < \xi_{0T}^2(\psi) \equiv 1 - \frac{B_0(\psi)}{B_{\max}(\psi)} \tag{49}$$

where $B_{\max}(\psi)$ is the maximum magnetic field on the flux-surface. For trapped electrons, the turning points $\theta_{\min}$ and $\theta_{\max}$ are then given by the positions where

$$B(\psi,0) = B_b(\psi,\xi_0) \equiv \frac{B_0(\psi)}{1-\xi_0^2} \tag{50}$$

For passing electrons, we can take simply $\theta_{\min} = 0$ and $\theta_{\max} = 2\pi$. The bounce or transit time is then given by

$$\tau_b(\psi,\xi_0) = \frac{2\pi R_p \tilde{q}(\psi)}{\upsilon|\xi_0|}\lambda(\psi,\xi_0) \tag{51}$$

where we define the normalized bounce time such that $\lambda = 1$ for electrons with $|\xi_0| = 1$:

$$\lambda(\psi,\xi_0) = \frac{1}{\tilde{q}(\psi)}\int_{\theta_{\min}}^{\theta_{\max}} \frac{d\theta}{2\pi}\,\frac{1}{|\hat{\psi}\cdot\hat{r}|}\,\frac{r}{R_p}\,\frac{B}{B_P}\,\frac{\xi_0}{\xi} \tag{52}$$

and

$$\tilde{q}(\psi) = \int_0^{2\pi} \frac{d\theta}{2\pi}\,\frac{1}{|\hat{\psi}\cdot\hat{r}|}\,\frac{r}{R_p}\,\frac{B}{B_P} \tag{53}$$

In equations (51)–(53), R_p is the major radius on axis, $B_p = |\nabla\psi|/R$ is the poloidal magnetic field and r is the local minor radius. The integral $\widetilde{q}$ coincides with the safety factor q in the large aspect ratio, low-β limit. The safety factor can also be calculated by numerical integration over θ

$$q(\psi) = \int_0^{2\pi} \frac{d\theta}{2\pi} \frac{1}{|\hat{\psi}\cdot\hat{r}|} \frac{r}{R} \frac{B_T}{B_P} \tag{54}$$

In order to reduce the kinetic equation, we define an integral over the particle orbit, called bounce averaging, by

$$\{\mathsf{A}\} = \frac{1}{\lambda\,\widetilde{q}} \left[\frac{1}{2}\sum_{\sigma}\right]_T \int_{\theta_{\min}}^{\theta_{\max}} \frac{d\theta}{2\pi} \frac{1}{|\hat{\psi}\cdot\hat{r}|} \frac{r}{R_p} \frac{B}{B_P} \frac{\xi_0}{\xi} \mathsf{A} \tag{55}$$

where the sum over $\sigma = \mathrm{sign}(\xi_0)$ applies to trapped electrons and accounts for both the forward and backward motion along banana orbits (within the thin banana width approximation). The bounce-averaging of kinetic operators, such as collisions, electric field, RF waves, etc, introduces other bounce integrals, which can be expressed in the form

$$\lambda_{k,l,m}(\psi,\xi_0) \equiv \lambda \left[\left(\frac{\xi}{\xi_0}\right)^k \Psi^l \left(\frac{R_0}{R(\psi,\theta)}\right)^m \right] \tag{56}$$

where ξ is defined in (47) and Ψ is defined in (48). Typically, numerical data from equilibrium codes give R, Z, B_R, B_Z, and B_ϕ on the (ψ,θ) grid. The evaluation of bounce integrals such as λ, $\lambda_{k,l,m}$, q, etc, can then be implemented numerically.

B. Reduction of the Drift Kinetic Equation

The DKE in an axisymmetric toroidal plasma is given by

$$\frac{\partial f}{\partial t} + \upsilon_{gc}\cdot\nabla f = \mathsf{C}(f) + \mathsf{Q}(f) + \mathsf{E}(f) \tag{57}$$

where $f = f(\psi,\theta,p,\xi,t)$ is the distribution function, $\mathsf{C}(f)$ is a FP collisions operator, $\mathsf{Q}(f)$ is a RF QL diffusion operator, and $\mathsf{E}(f)$ is a DC electric field operator. The guiding-center velocity υ_{gc} is decomposed into the parallel motion along the field line, and a drift velocity, as

$$\upsilon_{gc} = \upsilon_{\|}\hat{b} + \upsilon_D \tag{58}$$

The component of the drift velocity along the field lines can be neglected compared to the parallel velocity $\upsilon_{\|}$. The component across the flux-surfaces can be calculated either directly from the single particle drifts due to the magnetic field gradient and curvature, or from the conservation of toroidal canonical momentum. It is expressed as

$$\upsilon_D\cdot\nabla\psi = -\frac{\upsilon_{\|}}{\Omega} I(\psi)\, B\cdot\nabla\left(\frac{\upsilon_{\|}}{B}\right) \tag{59}$$

where Ω is the relativistic gyrofrequency. The DKE (57) becomes, in steady-state,

$$\upsilon_s \frac{\partial f}{\partial s} + \frac{\upsilon_{\|}}{\Omega} I(\psi) \frac{|\nabla\psi|}{R} \frac{\partial}{\partial s}\left(\frac{\upsilon_{\|}}{B}\right) \frac{\partial f}{\partial \psi} = \mathsf{C}(f) + \mathsf{Q}(f) + \mathsf{E}(f) \tag{60}$$

The characteristic time associated with the first term in this equation is clearly the bounce or transit time, while the time associated with the second term is the drift time. Typically, in high-temperature tokamaks,

the drift time τ_d is much longer than the bounce or transit time τ_b, and also much longer than the collisional time τ_e. We have therefore the following ordering

$$\delta_d = \frac{\tau_b}{\tau_d} << 1 \tag{61}$$

which is consistent with the small banana width approximation used in Section A. The DKE (60) is expanded in the small δ_d ordering as $f = f_0 + f_1 + \ldots$, which gives the set of equations (62)–(63)

$$\upsilon_s \frac{\partial f_0}{\partial s} = \mathsf{C}(f_0) + \mathsf{Q}(f_0) + \mathsf{E}(f_0) \tag{62}$$

$$\upsilon_s \frac{\partial f_1}{\partial s} + \frac{\upsilon_\parallel}{\Omega} I(\psi) \frac{|\nabla \psi|}{R} \frac{\partial}{\partial s}\left(\frac{\upsilon_\parallel}{B}\right) \frac{\partial f}{\partial \psi} = \mathsf{C}(f_1) + \mathsf{Q}(f_1) + \mathsf{E}(f_1) \tag{63}$$

In tokamaks, the bounce time is usually much shorter than the collisional detrapping time $\tau_{dt} = r\tau_e / R$. In this low-collisionality ($\nu^* = \tau_b / \tau_{dt} << 1$) regime, banana orbits are well-defined and the particle motion description of Section A is valid. In the zero-order DKE (62), the dominant term is therefore the motion along the field lines

$$\upsilon_s \frac{\partial f_0}{\partial s} = 0 \tag{64}$$

and f_0 is constant along the field lines. Bounce-averaging the equation (62), we then get an equation for $f_0 = f_0(\psi, p, \xi_0)$:

$$\{\mathsf{C}(f_0)\} + \{\mathsf{Q}(f_0)\} + \{\mathsf{E}(f_0)\} = 0 \tag{65}$$

In the low-collisionality regimes, the dominant terms in the first order DKE (63) are

$$\upsilon_s \frac{\partial f_1}{\partial s} + \frac{\upsilon_\parallel}{\Omega} I(\psi) \frac{|\nabla \psi|}{R} \frac{\partial}{\partial s}\left(\frac{\upsilon_\parallel}{B}\right) \frac{\partial f_0}{\partial \psi} = 0 \tag{66}$$

which integrates as

$$f_1 = \tilde{f} + g \tag{67}$$

where

$$\tilde{f} = \frac{\upsilon_\parallel}{\Omega} I(\psi) \frac{\partial f_0}{\partial \psi} \tag{68}$$

and g is an s- (or θ-)independent function. The equation for g is then obtained by bounce-averaging the equation (63):

$$\{\mathsf{C}(g)\} + \{\mathsf{Q}(g)\} + \{\mathsf{E}(g)\} = -\{\mathsf{C}(\tilde{f})\} - \{\mathsf{Q}(\tilde{f})\} - \{\mathsf{E}(\tilde{f})\} \tag{69}$$

To sum up, the total distribution function solution of the DKE expanded to first order in δ_d is

$$f = f_0 + \tilde{f} + g \tag{70}$$

where f_0 is the solution of the FP equation (65), in the presence of collisions, QL diffusion and DC electric field, but neglecting radial drifts; $\tilde{f}$ is a source term due to radial drifts (68), and g is the plasma response to these drifts in the presence of collisions, QL diffusion and DC electric field (69). In the absence of QL diffusion and DC electric field, f_0 is a Maxwellian and f_1 is the "bootstrap distribution function", meaning that the BC, generated by the radial drifts, is calculated by taking a moment of f_1.

C. DKE Solver

The reduced DKE is a set of two 2D momentum-space, second order, linear integro-differential equations with boundary condition on momentum space fluxes. These equations can be put in a the quasi-conservative form

$$\nabla_p \cdot S_p = \mathrm{I} \tag{71}$$

where the fluxes are decomposed into diffusive and convective parts

$$S_p = -\overline{\overline{D}}_p \nabla_p f + F_p f \tag{72}$$

and I is an integral term resulting from the collisions operator. Because this integral term is a small contribution to the equation, it is treated explicitly while the differential term is solved implicitly. In addition, the symmetrization of the distribution function in the trapped region is also treated implicitly,[23] which leads to extremely fast convergence of the DKE code.

The equation is solved on non-uniform grids, which allows more precise calculations in the significant regions of momentum space, for example in the vicinity of the trapped/passing boundary.

The code has been benchmarked against other models and codes for the calculation of the BC, the neoclassical conductivity and RFCD. An example of BC calculation in Alcator C-Mod is shown in Figure 6, where the results from our kinetic code are compared to fluid models.[24,25]

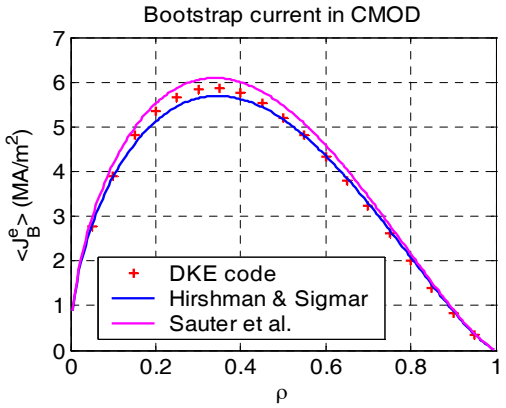

Figure 6: Bootstrap current in Alcator C-Mod. The results from our DKE code are compared with various fluid models.[24,25]

[23] J. Killeen, G. D. Kerbel, M. G. McCoy, and A. A. Mirin, *Computational Methods for Kinetic Models of Magnetically Confined Plasmas* (New York: Springer-Verlag), 1986.
[24] S.P. Hirshman and D.J. Sigmar, "Neoclassical Transport of Impurities in Tokamak Plasmas," *Nucl. Fus.* 21(9), 1079–1201 (1981).
[25] O. Sauter, C. Angioni, and Y. R. Lin-Liu, "Neoclassical Conductivity and Bootstrap Current Formulas for General Axisymmetric Equilibria and Arbitrary Collisionality Regime," *Phys. Plasmas* 6(7), 2834–2839 (1999).

D. Moments of the Distribution Function

In order to study RFCD and the synergism between RFCD and the BC, we need to calculate moments of the distribution function, in particular the flux-surface averaged current density and density of power absorbed.

The flux-surface averaged toroidal current density associated with the θ-independent functions f_0 and g is given by

$$\left\langle J_{\parallel}\right\rangle_{\phi}^{0}(\psi)=\frac{2\pi\, q_e}{m}\ \frac{q}{\bar{=}{q}}\int_0^{\infty}dp\,\frac{p^3}{\gamma}\int_{-1}^{1}\ d\xi_0\xi_0 f(p,\xi_0,\psi) \tag{73}$$

with

$$\bar{=}{q}(\psi)\equiv\int_0^{2\pi}\frac{d\theta}{2\pi}\ \frac{1}{|\,\hat{\psi}\cdot\hat{r}\,|}\ \frac{r}{R}\ \frac{B_0}{B_P} \tag{74}$$

The flux-surface averaged toroidal current associated with $\widetilde{f}$ is

$$\left\langle \widetilde{J}_{\parallel}\right\rangle_{\phi}^{1}(\psi)=\frac{2\pi\, q_e}{m}\ \frac{\widetilde{q}}{\bar{=}{q}}\ \frac{R_p}{R_0}\ \frac{B_{T0}}{B_0}\int_0^{\infty}dp\,\frac{p^3}{\gamma}\ \int_{-1}^{1}\ d\xi_0\lambda_{2,-2,2}\xi_0\widetilde{f}^{(0)}(p,\xi_0,\psi) \tag{75}$$

where

$$\widetilde{f}^{(0)}(p,\xi_0,\psi)=\frac{\Psi\xi_0}{\xi}\ \widetilde{f}(p,\xi_0,\psi,\theta) \tag{76}$$

The density of power absorbed corresponding to any momentum space operator O, such as C, Q, or E, is

$$\left\langle P_{abs}^{\mathsf{O}}\right\rangle_V(\psi)=2\pi\ \frac{\widetilde{q}(\psi)}{\hat{q}(\psi)}\int_0^{\infty}dp\,\frac{p^3}{\gamma\, m_e}\int_{-1}^{+1}\ d\xi_0\lambda\{S_p^{\mathsf{O}}\} \tag{77}$$

where

$$\hat{q}(\psi)\equiv\int_0^{2\pi}\frac{d\theta}{2\pi}\ \frac{1}{|\,\hat{\psi}\cdot\hat{r}\,|}\ \frac{r}{R_p}\ \frac{B_0}{B_P} \tag{78}$$

and S_p^{O} is the projection, in the direction of the momentum p, of the momentum-space flux S_p (72) associated with the operator O.

E. Conclusion

We have developed a numerical code which solves the DKE in arbitrary tokamak geometry with no approximation on the aspect ratio and arbitrary plasma β. This code will allow us to calculate RFCD and Ohmic CD self-consistently with the bootstrap current and study possible synergisms. In particular, future work using this new code will extend our study of Electron Bernstein Wave (EBW) CD[26] in ST to include the effect of realistic geometries and the synergism with the BC.

[26] J. Decker, A. K. Ram, A. Bers, and Y. Peysson, "Plasma Electrodynamics and Applications: Section 3 – Ohkawa Current Drive by Electron Bernstein Waves in Spherical Tori," *Progress Report No. 146,* MIT Research Laboratory of Electronics, Cambridge, 2004.

5. Development of the 1-Dimensional Collisionless Kinetic Code ELVIS

Sponsors
Department of Energy (DoE) Contract DE-FG02-91ER-54109

Project Staff
D. J. Strozzi, Professor A. Bers, Dr. A. K. Ram

Unlike conventional fluids, which are dominated by particle collisions, plasmas frequently are sufficiently hot or low-density that collisions play a small role in the dynamics. In collisionless regimes, kinetic descriptions of the plasma that follow the distribution of particles in both position and velocity space are sometimes necessary. For instance, linear electrostatic plasma waves experience collisionless Landau damping, which fluid theory does not predict. Laser-plasma interactions lead to parametric instabilities which couple electromagnetic waves to electrostatic waves.[27] As these instabilities grow, the electrostatic fluctuations reach large amplitudes. Kinetic effects may therefore be important in their saturation. We have developed a code called ELVIS (Eulerian VLasov Integrator with Splines) that solves for the 1-dimensional time evolution of a plasma with longitudinal and transverse electromagnetic fields.

We give the governing equations for the Vlasov-Maxwell system in Section A. Section B presents our numerical scheme for evolving the system in time. We present benchmarks of the code on periodic, electrostatic (no transverse fields) electron plasma waves in Section C. In particular, we explore Landau damping, trapping, and wave-breaking behavior.

A. Governing Equations

We consider a plasma that varies only in x $(\partial/\partial y = \partial/\partial z = 0)$. The plasma interacts with a longitudinal electrostatic field E_x and transverse electromagnetic fields E_y and B_z (linearly polarized in the y direction). We treat the particles as a cold fluid in the y direction, all with the same transverse velocity $v_y(x,t)$. This transverse flow couples the longitudinal (x) and transverse (y,z) dynamics.

The Vlasov equation describes the collisionless evolution of the distribution function $f_s(x, p_x, t)$ for each particle species s in the x direction:

$$\frac{\partial f_s}{\partial t} + v_x \frac{\partial f_s}{\partial x} + F_{xs} \frac{\partial f_s}{\partial p_x} = 0 \qquad F_{xs} = eZ_s(E_x + v_{ys} B_z) \tag{79}$$

The velocity $v_x = p_x / m_s$ nonrelativistically and $v_x = p_x/(\gamma_s m_s)$ relativistically, where $\gamma_s = \sqrt{1 + (p_x / m_s c)^2}$. F_{xs} is the electromagnetic force acting on the particles in the x-direction, e is the positron charge, and Z_s is the species charge state. Fluid quantities are found by taking moments of f_s. For example, the number density n_s is

$$n_s = \int_{-\infty}^{\infty} dp_x \, f_s(x, p_x, t) \tag{80}$$

The longitudinal electric field E_x is related to the charge density ρ by Gauss' law:

$$\frac{\partial E_x}{\partial x} = \varepsilon_0^{-1} \rho \qquad \rho = e \sum\nolimits_s Z_s n_s \tag{81}$$

[27] W. L. Kruer, *The Physics of Laser Plasma Interactions* (Redwood City, California: Addison-Wesley), 1988.

The transverse fields E_y and B_z are found by forming the right- and left-moving combinations E^+ and E^-:

$$E^{\pm} = E_y \pm cB_z \qquad \left(\frac{\partial}{\partial t} \pm c\frac{\partial}{\partial x}\right)E^{\pm} = -\varepsilon_0^{-1} J_y \tag{82}$$

$J_y = e\sum_s Z_s n_s v_{ys}$ is the transverse current. The evolution equations for $E^{\pm}$ come from Ampere's law.

The transverse momentum equation is given by conservation of canonical y momentum, taken to be zero initially:

$$m_s \frac{\partial v_{ys}}{\partial t} = q_s E_y \tag{83}$$

B. Numerical Method

In this section we describe how we advance the system by one timestep from t_n to t_{n+1}, where $t_n = n\,dt$. We do this in a leapfrog manner. We evolve f by splitting the Vlasov equation into advection equations in space and momentum and solving each along characteristics. This method was first used by Cheng and Knorr for the electrostatic Vlasov-Poisson system.[28] We follow Ghizzo et al's extension[29] of scheme to the electromagnetic, Vlasov-Maxwell system. Unlike them, we use cubic splines for the interpolation involved in the spatial free-streaming of f rather than Fourier transforms.

(i). Time Evolution of f

The Vlasov equation states that f (we suppress species subscript s when there is no confusion) is constant along its characteristics, or the particle orbits. The orbits are the paths $[X(t), P_x(t)]$ in phase space described by

$$\frac{dX}{dt} = V_x, \qquad \frac{dP_x}{dt} = F_x \tag{84}$$

The time-splitting method entails alternately solving a free-streaming and acceleration equation:

$$\frac{\partial f}{\partial t} + v_z \frac{\partial f}{\partial x} = 0 \qquad \frac{\partial f}{\partial t} + F_x \frac{\partial f}{\partial p_x} = 0 \tag{85}$$

Each equation is an advection equation, with characteristics along which f is constant. The characteristics of the free-streaming equation are

$$X = X_0 + V_{x0}\,t, \qquad P_x = P_{x0} \tag{86}$$

Free-streaming therefore amounts to shifting f in space:

$$f(x, p_x, t + dt) = f(x - v_x\,dt, p_x, t) \tag{87}$$

Similarly, the acceleration step gives

$$f(x, p_x, t + dt) = f(x, p_x - F_x dt, t) \tag{88}$$

[28] C. Z. Cheng and G. Knorr, "The Integration of the Vlasov Equation in Configuration Space," *Jour. Comp. Phys.* 22(3): 330–351 (1976).

[29] A. Ghizzo, P. Bertrand, M. M. Shoucri, T. W. Johnston, E. Fijalkow, and M. R. Feix, "A Vlasov Code for the Numerical Simulation of Stimulated Raman Scattering," *Jour. Comp. Phys.* 90(2): 431–457 (1990).

We can picture this as turning the force into a series of kicks applied at the timesteps t_n and zero otherwise. This requires $\rho(t_n)$ to compute E_x, as well as $E^{\pm}(t_n)$. Following Ghizzo, we use a leapfrog scheme to interleave the time evolution of the longitudinal and transverse fields. They have shown this approach to be accurate to order dt.[28]

We advance f for a whole timestep by alternating a half free stream, a full acceleration, and a half free stream. We advance f from $t_{n-1/2}$ to $t_{n+1/2}$ as follows:

$$\begin{aligned} f(x,p_x,t_{n^-}) &= f(x - v_x\,dt/2, p_x, t_{n-1/2}) \qquad \text{half-stream}\,(\mathrm{S}_{1/2}) \\ f(x,p_x,t_{n^+}) &= f(x, p_x - F\,dt, t_{n^-}) \qquad \text{accelerate}\,(\mathrm{A}) \\ f(x,p_x,t_{n+1/2}) &= f(x - v_x\,dt/2, p_x, t_{n^+}) \qquad \text{half-stream}\,(\mathrm{S}_{1/2}) \end{aligned} \tag{89}$$

By arranging the time evolution so the first and last steps are both half-streams, we can combine these into a single stream for a full timestep dt (denoted S in Figure 7). We must first take a special initial time-step to setup the system appropriately for this.

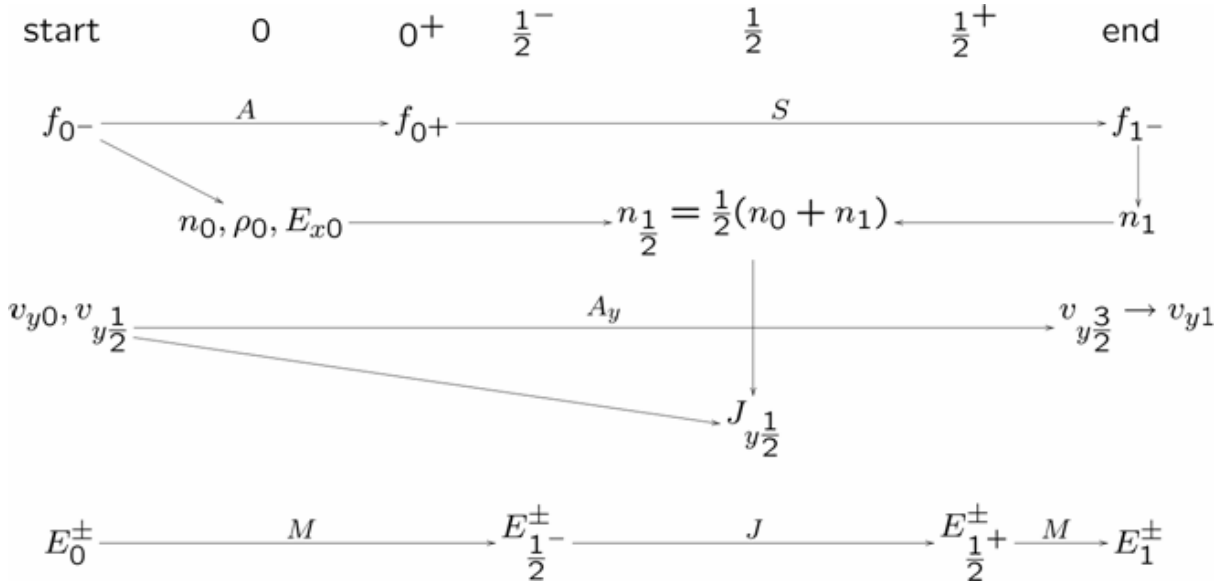

Figure 7: Schematic of ELVIS time evolution algorithm.

(ii). Gauss' Law

We solve Gauss' Law for E_x in Fourier space. Given $\rho(x)$ we compute its Fourier transform $\rho(k)$. From this we find the Fourier transform of E_x, $E(k) = \rho(k)/ik$, and set $E(k=0) = 0$. We then inverse Fourier transform to find $E_x(x)$. We still have to choose the DC component of E_x, which corresponds to the boundary condition needed in Gauss' law. The code provides for two choices:

1. Short-circuit boundary condition: This choice comes from demanding the potential ϕ be periodic, where $E_x = -\partial\phi/\partial x$ If we integrate this equation over the box, we find

$$\int_0^L dx E_x = \phi(0) - \phi(L) = 0 \tag{90}$$

We therefore offset E_x so that its average is zero.

2. Finite boundary condition: We imagine for this case a plasma of finite extent, surrounded by an infinite vacuum region. In the code, the initial density profile is localized in x, so that there are regions of zero density between the box edges an the plasma. As long as the density remains sufficiently small near the edges, we may consider it as periodic $[n(0) = n(L) = 0]$. It is therefore acceptable to use the Fourier method, since E_x is periodic if n is. We do not want particles in the low-density edges to feel an appreciable E_x. This could happen is we use the short-circuit boundary condition. Instead, we set $E_x(x = 0) = 0$. Since the plasma is periodic, $E_x(x = L)$ should be zero as well. This will be the case if the system has no net charge, as can be seen by integrating Gauss' law over the box.

(iii). Advancing Transverse Fields v_{ys} and $E^{\pm}$

We advance v_{ys} from $t_{n+1/2}$ to $t_{n+3/2}$ using a forward-Euler step with the force $q_s E_y$ coming from $E^{\pm}$ at t_{n+1}:

$$v_{ys}\left(t_{n+\frac{3}{2}}\right) = v_{ys}\left(t_{n+\frac{1}{2}}\right) + \frac{q_s\, dt}{2 m_s}\left(E^{+}(t_{n+1}) + E^{-}(t_{n+1})\right) \qquad \text{accelerate in y } (\mathrm{A_y}) \tag{91}$$

The advection equations for $E^{\pm}$ are analogous to the Vlasov equation. As with the force F in the Vlasov equation, we view the source J_y as a series of kicks acting at the half-timesteps $t_{n+1/2}$. The staggering of the kicks at the full timesteps for f and half-timesteps for $E^{\pm}$ is part of the leapfrog technique.

Advancing $E^{\pm}$ from t_n to t_{n+1} is performed as follows:

$$\begin{aligned} E^{\pm}\left(t_{n+1/2^-}, x\right) &= E^{\pm}\left(t_n, x \mu\, dt/2\right) && \text{Maxwell free - stream (M)} \\ E^{\pm}\left(t_{n+1/2^+}\right) &= E^{\pm}\left(t_{n+1/2^-}\right) - \tfrac{1}{2\varepsilon_0} J_y\left(t_{n+1/2}\right) && \text{current source (J)} \\ E^{\pm}\left(t_{n+1}, x\right) &= E^{\pm}\left(t_{n+1/2^+}, x \mu\, dt/2\right) && \text{Maxwell free - stream (M)} \end{aligned} \tag{92}$$

Figure 7 sketches how we advance the system for one timestep, from $n = 0$ to $n = 1$:

C. Results for Electrostatic Problems

Before proceeding to electromagnetic problems, we use ELVIS in its electrostatic (no transverse fields), periodic mode with fixed ions and the short-circuit boundary condition for Gauss' law. This is useful for studying the evolution of electron plasma waves (EPWs) both linearly and nonlinearly. The linear dispersion relation for EPWs in a Maxwellian f_e is given by the complex ω roots for real k of

$$\varepsilon = 1 + \chi_e = 1 - \frac{1}{2k^2 \lambda_{De}^{\ 2}} Z'\left(\frac{\omega}{|k| v_{Te}\sqrt{2}}\right) = 0 \tag{93}$$

$\lambda_{De} = (\varepsilon_0 T_e / n_0 e^2)^{1/2}$ is the electron Debye length, $v_{Te} = (T_e / m_e)^{1/2}$ is the electron thermal speed, $Z(\zeta) = i\sqrt{\pi} e^{-\zeta^2} \mathrm{erfc}(i\zeta)$ is the plasma dispersion function, and the Maxwellian equilibrium f_e is

$$f_e = \frac{n_0}{v_{Te}\sqrt{2\pi}} e^{-v^2/2v_{Te}^2} \tag{94}$$

For $k\lambda_{De} << 1$, this gives

$$\omega = \omega_r + i\omega_i \qquad \left(\frac{\omega_r}{\omega_{pe}}\right)^2 = 1 + 3(k\lambda_{De})^2 \qquad \frac{\omega_i}{\omega_{pe}} = -\sqrt{\frac{\pi}{8}} e^{-3/2} |k\lambda_{De}|^{-3} e^{-\frac{1}{2}(k\lambda_{De})^{-2}} \tag{95}$$

$\omega_{pe} = (n_0 e^2 / \varepsilon_0 m_e)^{1/2}$ is the electron plasma frequency. The imaginary part of ω represents collisionless Landau damping of the wave.

A single traveling EPW involves perturbations to the density, bulk flow, and electric field given by

$$n_1 = \alpha n_0 \sin\psi \qquad v_1 = \alpha \frac{\omega}{k} \sin\psi \qquad E_1 = \alpha \frac{n_0 e}{\varepsilon_0 k} \cos\psi \qquad \psi = kx - \omega t \tag{96}$$

We impose an EPW in the initial conditions by perturbing just the density and not the velocity. This corresponds to a standing EPW, or two traveling EPWs moving in opposite directions.

Figure 8 shows E_x vs. time at a fixed x in an electrostatic run with an initial standing EPW density perturbation corresponding to $k\lambda_{De} = 0.3$ and amplitude $\alpha = 10^{-3}$. The blue points are simulation results and the red curve is a best-fit damped harmonic given by $E_{\mathrm{fit}}(t) = E_0 + E_1 \sin[\omega(t - t_0)\exp[-\nu(t - t_0)]$. The fitted values are $\omega = 1.160$ and $\nu = 0.01257$ and match very nicely with the numerical roots of the kinetic dispersion relation $\omega = 1.160$ and $\nu = 0.01262$. The fit is for $\omega_p t = 10$ to 100. We exclude the start of the run since phase-mixing reduces the wave amplitude more than Landau damping for the first oscillation. The fitted offset and amplitude are $E_0 = -1.4 \cdot 10^{-9}$ and $E_1 = 7.4 \cdot 10^{-5}$

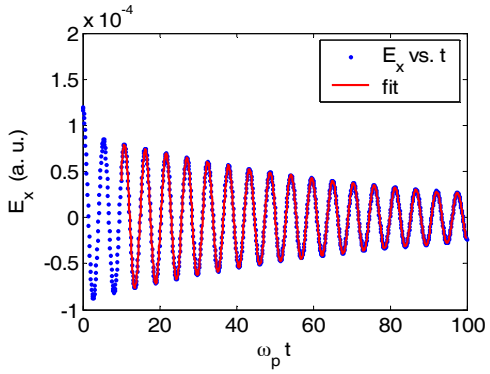

Figure 8: E_x vs. t at a fixed x. $k\lambda_{De} = 0.3$ and $\alpha = 10^{-3}$. The red fit has $\omega = 1.160\omega_{pe}$ and $\nu = 0.01257\omega_{pe}$.

A nonlinear treatment of the time evolution of EPWs shows that the wave amplitude does not decay indefinitely, but instead oscillates and eventually reaches a constant value.[30] This occurs because particles trapped in the potential well of the wave bounce back and forth, first receiving energy from and then giving energy back to the wave. The time scale for bouncing is related to the bounce frequency $\omega_b = (eE_0 k / m_e)^{1/2}$ of particles trapped in the wave. The instantaneous damping rate matches the Landau value for early times $\omega_b t << 1$, followed by oscillation, and asymptotically approaches zero for $\omega_b t >> 1$.

Figure 9 compares the time evolution of the electric field amplitude given by Landau damping, O'Neil's calculation, and ELVIS simulations. Initially, the phase-mixing of initial conditions gives a more rapid loss of wave energy than the Landau rate. This is most apparent in the case $\alpha = 0.1$. After this, Landau damping occurs until the trapped particles bounce and the wave amplitude oscillates. The wave loses more energy than O'Neil predicts, since his derivation assumes a fixed wave amplitude. As the wave damps, some initially trapped particles become untrapped and do not give back all the energy they gain to the wave. In addition, $\omega_b \sim E^{1/2}$, so as the wave damps the trapped particles take longer to bounce. This explains why the amplitude bounces more slowly in the self-consistent simulations than in O'Neil's theory.

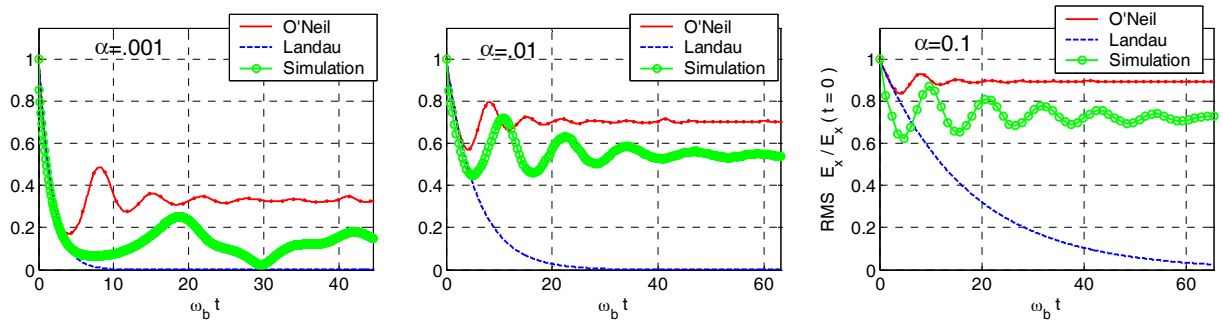

Figure 9: Nonlinear amplitude oscillation of $E_x(t)$ at fixed x in standing EPW. $k\lambda_{De} = 0.3$.

Not only the damping rate but the frequency of the EPW oscillates in time due to the finite wave amplitude.[31] Morales calculates the frequency shift $\delta\omega(t) = \omega(t) - \omega_L$ to be

$$\delta\omega = -1.63\,\Omega_0\, g(t) \qquad \Omega_0 = \sqrt{\alpha}\left(\frac{\omega_{pe}}{k}\right)^3 \frac{1}{n_0} f_0''(v_p)\left(\frac{\partial\varepsilon}{\partial\omega}\right)^{-1} \omega_L \tag{97}$$

$\omega(t)$ is the actual time-dependent real frequency, ω_L is the real frequency from the linear dispersion relation [given by Eq. (93) or, approximately, by (95)]. ε is the dielectric function $g(t)$ is a function that oscillates on the bounce time scale, $g(0) = 0$, and $g(\infty) = 1$.

For a Maxwellian f_0 as in Eq. (94) in the fluid limit $v_p >> v_{Te}$, this becomes

[30] T. O'Neil, "Collisionless Damping of Nonlinear Plasma Oscillations," *Phys. Fluids* 8(12): 2255–2262 (1965).
[31] G. J. Morales and T. M. O'Neil, "Nonlinear Frequency Shift of an Electron Plasma Wave," *Phys. Rev. Lett.* 28(7): 417–420 (1972).

$$\frac{\Omega_0}{\omega_L} = \frac{1}{\sqrt{8\pi}} \frac{\alpha^{1/2}}{k\lambda_{De}} a^{-2} \frac{1-a}{1+\frac{15}{2}a} e^{-1/(2a)} \qquad a \equiv \left(\frac{v_{Te}}{v_p} \right)^2 \tag{98}$$

We can find $\omega(t)$ for a simulation by splitting $E_x(t)$ at a fixed x into temporal bins of several linear wave periods, and fitting E_x with $E_{\text{fit}} = E_0 + E_1(1+bt+ct^2)\sin[\omega(t-t_0)]$. This gives us the best-fit frequency in each bin, and accounts for the slow change in amplitude via b and c.

Figure 10 shows $\delta\omega/\omega_L$ from this fitting procedure. We see that Morales overstates the frequency shift $\delta\omega$ compared to the simulations. For each of the three cases shown, the numerical $\delta\omega$ is about 2/3 Morales' value. The observed $\delta\omega$ scales as $\alpha^{1/2}$ and is negative, as predicted by Morales.

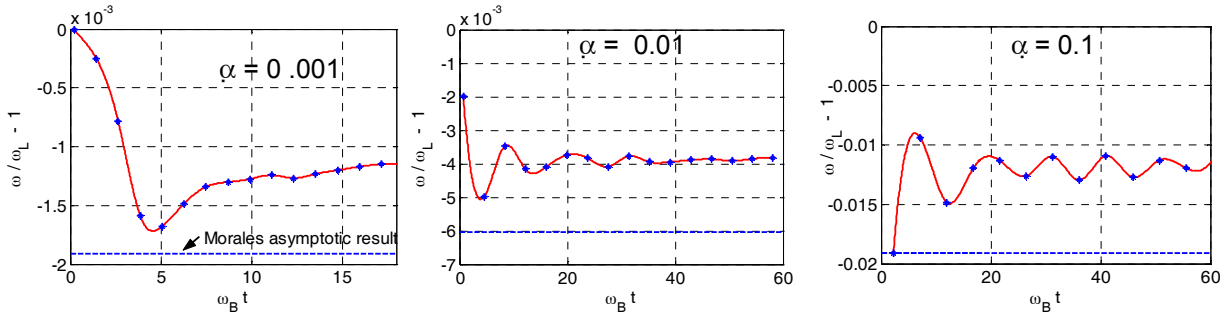

Figure 10: Fitted frequency shift $\delta\omega(t)$ for an initial standing EPW of amplitude α and $k\lambda_{De} = 0.3$.

There is a maximum amplitude for coherent, periodic EPWs, called the wavebreaking limit. This has been derived analytically for the cold-relativistic,[32] cold-nonrelativistic,[33] warm-nonrelativistic,[34] and warm-relativistic[35,36] fluids models. A simple way to understand wavebreaking is the over-taking of slow particles by fast particles. A fluid model treats averaged, "bulk" quantities of the plasma particles as functions of time and space: the density, flow, etc. If the flow in a periodic wave is large enough, fast fluid may "out-run" the fluid in front of it before the wave oscillates. This would lead to two flow values at one x, which is impossible in a fluid model. Kinetic models, which follow the number of particles at each location with each velocity, do not break down in this way. The physical importance of wavebreaking in a kinetic description is that waves above this threshold rapidly lose energy and heat the particles.

Figure 11(a) displays the wavebreaking limit for a warm, nonrelativistic plasma derived by Coffey. Increasing the temperature increases v_{Te}/v_p and lowers the wavebreaking limit below the cold value found by Dawson (to which $E_{\max}$ is normalized in the figure). Finite temperature gives rise to a pressure, which opposes the formation of high density regions in the wave.

[32] A. I. Akhiezer and R. V. Polovin, "Theory of Wave Motion of an Electron Plasma," *Soviet Physics–JETP* 3(5): 696–705 (1956).
[33] J. M. Dawson, "Nonlinear Electron Oscillations in a Cold Plasma," *Phys. Rev.* 113(2): 383–387 (1959).
[34] T. P. Coffey, "Breaking of Large Amplitude Plasma Oscillations," *Phys. Fluids* 14(7): 1402–1406 (1971).
[35] T. Katsouleas and W. B. Mori, "Wave-Breaking Amplitudes of Relativistic Oscillations in a Thermal Plasma," *Phys. Rev. Lett.* 61(1): 90–93 (1988).
[36] W. B. Mori and T. Katsouleas, "Wavebreaking of Longitudinal Plasma Oscillations," *Physica Scripta* T30: 127–133 (1990).

One way to see the wavebreaking dynamics is to consider the long-time evolution of a wave present in the initial conditions. Linear kinetic theory predicts the wave is Landau damped. However, we have seen that for moderate amplitudes the wave energy oscillates with some overall decrease in energy, as calculated by O'Neil and verified in ELVIS simulations. As the wave amplitude increases beyond the range of validity for O'Neil, the phase-space vortices start to trap bulk distribution particles far from the wave's phase velocity. This rapidly heats the particles, and lowers the wave amplitude.

Let us see how this plays out for initial traveling EPWs as we increase the amplitude. Figure 11(b) shows the ratio of final to initial electric-field energy $W = (\varepsilon_0 / 2)E_x^2$ for waves of different initial amplitude. For these waves $k\lambda_{De} = 0.2$, giving very weak Landau damping $(\omega_1 / \omega_{pe} = -5.5 \cdot 10^{-5})$. O'Neil's theory predicts that for all the amplitudes shown, trapped particles bounce so quickly that the wave loses essentially no energy. However, numerical simulations show an appreciable fraction of energy is lost, and this fraction increases with initial amplitude. This reveals a nonlinear mechanism that transfers energy from the wave to the particles.

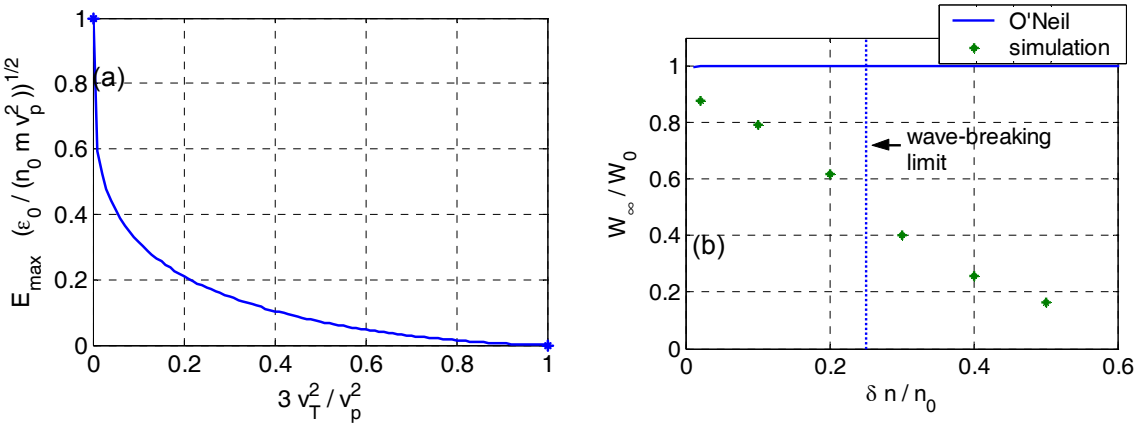

Figure 11: (a) Coffey's wavebreaking electric field amplitude. $E_{\max}$ is scaled by Dawson's cold wavebreaking value. (b) Ratio of final to initial electric-field energy in ELVIS simulations of a traveling EPW with $k\lambda_{De} = 0.2$ and different amplitudes.

Publications

Journal Articles, Published

B. Jones, P. C. Efthimion, G. Taylor, T. Munsat, J. R. Wilson, J. C. Hosea, R. Kaita, R. Majeski, R. Maingi, S. Shiraiwa, J. Spaleta, and A. K. Ram, “Controlled Optimization of Mode Conversion from Electron Bernstein Waves to Extraordinary Mode in Magnetized Plasma," *Phys. Rev. Lett.* 90(16): 165001/1-4 (2003).

D. Mueller, M. Ono, M. G. Bell, R. E. Bell, M. Bitter, C. Bourdelle, D. S. Darrow, P. C. Efthimion, E. D. Fredrickson, D. A. Gates, R. J. Goldston, L. R. Grisham, R. J. Hawryluk, K. W. Hill, J. C. Hosea, S. C. Jardin, H. Ji, S. M. Kaye, R. Kaita, H. W. Kugel, D. W. Johnson, B. P. LeBlanc, R. Majeski, E. Mazzucato, S. S. Medley, J. E. Menard, H. K. Park, S. F. Paul, C. K. Phillips, M. H. Redi, A. L. Rosenberg, C. H. Skinner, V. A. Soukhanovskii, B. Stratton, E. J. Synakowski, G. Taylor, J. R. Wilson, S. J. Zweben, W. D. Dorland, Y. K. M. Peng, R. Barry, T. Bigelow, C. E. Bush, M. Carter, R. Maingi, M. Menon, P. M. Ryan, D. W. Swain, J. Wilgen, S. A. Sabbagh, F. Paoletti, J. Bialek, W. Zhu, R. Raman, T. R. Jarboe, B. A. Nelson, R. J. Maqueda, G. A. Wurden, R. I. Pinsker, M. Schaffer, J. Ferron, L. Lao, D. Stutman, M. Finkenthal, W. Wampler, S. Kubota, W. A. Peebles, M. Gilmore, T. K. Mau, K. C. Lee, C. W. Domier, B. H. Deng, M. Johnson, N. C. Luhmann, Jr., P. Bonoli, A. Bers, A. Ram, R. Akers, Y. Takase, A. Ejiri, Y. Ono, S. Shiraiwa, N. Nishino, O. Mitarai, M. Nagata, J. G. Yang, H. Na, and D. Pacella, “Results of NSTX Heating Experiments," *IEEE Trans. Plasma Sci.* 31(1), 60–67 (2003).

M. Ono, M. G. Bell, R. E. Bell, T. Bigelow, M. Bitter, W. Blanchard, J. Boedo, C. Bourdelle, C. Bush, W. Choe, J. Chrzanowski, D. S. Darrow, S. J. Diem, R. Doerner, P. C. Efthimion, J. R. Ferron, R. J. Fonck, E. D. Fredrickson, G. D. Garstka, D. A. Gates, T. Gray, L. R. Grisham, W. Heidbrink, K. W. Hill, D. Hoffman, T. R. Jarboe, D. W. Johnson, R. Kaita, S. M. Kaye, C. Kessel, J. H. Kim, M. W. Kissick, S. Kubota, H. W. Kugel, B. P. LeBlanc, K. Lee, S. G. Lee, B. T. Lewicki, S. Luckhardt, R. Maingi, R. Majeski, J. Manickam, R. Maqueda, T. K. Mau, E. Mazzucato, S. S. Medley, J. Menard, D. Mueller, B. A. Nelson, C. Neumeyer, N. Nishino, C. N. Ostrander, D. Pacella, F. Paoletti, H. K. Park, W. Park, S. F. Paul, Y-K. M. Peng, C. K. Phillips, R. Pinsker, P. H. Probert, S. Ramakrishnan, R. Raman, M. Redi, A. L. Roquemore, A. Rosenberg, P. M. Ryan, S. A. Sabbagh, M. Schaffer, R. J. Schooff, R. Seraydarian, C. H. Skinner, A. C. Sontag, V. Soukhanovskii, J. Spaleta, T. Stevenson, D. Stutman, D .W. Swain, E. Synakowski, Y. Takase, X. Tang, G. Taylor, J. Timberlake, K .L. Tritz, E. A. Unterberg, A. Von Halle, J. Wilgen, M. Williams, J. R. Wilson, X. Xu, S. J. Zweben, R. Akers, R. E. Barry, P. Beiersdorfer, J. M. Bialek, B. Blagojevic, P. T. Bonoli, M. D. Carter, W. Davis, B. Deng, L. Dudek, J. Egedal, R. Ellis, M. Finkenthal, J. Foley, E. Fredd, A. Glasser, T. Gibney, M. Gilmore, R. J. Goldston, R. E. Hatcher, R. J. Hawryluk, W. Houlberg, R. Harvey, S. C. Jardin, J. C. Hosea, H. Ji, M. Kalish, J. Lowrance, L. L. Lao, F. M. Levinton, N. C. Luhmann, R. Marsala, D. Mastravito, M. M. Menon, O. Mitarai, M. Nagata, G. Oliaro, R. Parsells, T. Peebles, B. Peneflor, D. Piglowski, G. D. Porter, A. K. Ram, M. Rensink, G. Rewoldt, J. Robinson, P. Roney, K. Shaing, S. Shiraiwa, P. Sichta, D. Stotler, B. C. Stratton, R. Vero, W. R. Wampler, and G. A. Wurden, “Progress Towards High-Performance, Steady-State Spherical Torus,” *Plasma Phys. Contr. Fus.* 45(12A): A335–A350 (2003). Online paper A335, December 2003, http://www.iop.org/EJ/toc/0741-3335/45/12A (January 14, 2004).

A. K. Ram and A. Bers, “Excitation and Emission of Electron Cyclotron Waves in Spherical Tori,” *Nucl. Fusion* 43(11): 1305–1312 (2003).

A. Salcedo, R. J. Focia, A. K. Ram, and A. Bers, “Studies of Stimulated Raman Back-Scattering and Associated Nonlinear Laser Plasma Interactions,” *Nucl. Fusion* 43(12): 1759–1770 (2003).

D. J. Strozzi, A. K. Ram, and A. Bers, “Coherent Acceleration of Magnetized Ions by Electrostatic Waves With Arbitrary Wavenumbers," *Phys. Plasmas* 10(7): 2722–2731 (2003).

E. J. Synakowski, M. G. Bell, R. E. Bell, T. Bigelow, M. Bitter, W. Blanchard, J. Boedo, C. Bourdelle, C. Bush, D. S. Darrow, E. D. Fredrickson, D. A. Gates, M. Gilmore, L. R. Grisham, J. C. Hosea, D. W. Johnson, R. Kaita, S. M. Kaye, S. Kubota, H. W. Kugel, B. P. LeBlanc, K. Lee, R. Maingi, J. Manickam, R.

Maqueda, E. Mazzucato, S. S. Medley, J. Menard, D. Mueller, B. A. Nelson, C. Neumeyer, M. Ono, F. Paoletti, H. K. Park, S. F. Paul, Y.-K. M. Peng, C. K. Phillips, S. Ramakrishnan, R. Raman, A. Rosenberg, P. M. Ryan, S. A. Sabbagh, C. H. Skinner, V. Soukhanovskii, T. Stevenson, D. Stutman, D. W. Swain, G. Taylor, A. Von Halle, J. Wilgen, M. Williams, J. R. Wilson, S. J. Zweben, X. Xu, R. Akers, R. E. Barry, P. Beiersdorfer, J. M. Bialek, B. Blagojevic, P. T. Bonoli, R. Budny, M. D. Carter, J. Chrzanowski, W. Davis, B. Deng, E. J. Doyle, L. Dudek, P. C. Efthimion, J. Egedal, R. Ellis, J. R. Ferron, M. Finkenthal, J. Foley, E. Fredd, A. Glasser, T. Gibney, R. J. Goldston, R. Harvey, R. E. Hatcher, R. J. Hawryluk, W. Heidbrink, K. W. Hill, W. Houlberg, T. R. Jarboe, S. C. Jardin, H. Ji, M. Kalish, J. Lawrance, L. L. Lao, K. C. Lee, F. M. Levinton, N. C. Luhmann, R. Majeski, R. Marsala, D. Mastravito, T. K. Mau, B. McCormack, M. M. Menon, O. Mitarai, M. Nagata, N. Nishino, M. Okabayashi, G. Oliaro, D. Pacella, R. Parsells, T. Peebles, B. Peneflor, D. Piglowski, R. Pinsker, G. D. Porter, A. K. Ram, M. Redi, M. Rensink, G. Rewoldt, J. Robinson, P. Roney, A. L. Roquemore, M. Schaffer, K. Shaing, S. Shiraiwa, P. Sichta, D. Stotler, B. C. Stratton, Y. Takase, X. Tang, R. Vero, W. R. Wampler, G. A. Wurden, X. Q. Xu, J. G. Yang, L. Zeng, and W. Zhu, “The National Spherical Torus Experiment (NSTX) Research Program and Progress Towards High Beta, Long Pulse Operating Scenarios,” *Nucl. Fusion* 43(12): 1653–1664 (2003).

Journal Articles, Submitted for Publication

D. J. Strozzi, M. Shoucri, and A. Bers, “Study of Laser Plasma Interactions Using an Eulerian Vlasov Code,” to appear in *Comp. Phys. Comm.* (2004).

Meeting Papers, Published

J. Decker, “ECCD for Advanced Tokamak Operations Fisch-Boozer versus Ohkawa Methods,” *Proc. 15th Topical Conference on Radio Frequency Power in Plasmas*, Moran, Wyoming, May 19–21, 2003. A.I.P. Conf. Proc. 694 (ed. C. B. Forest), Melville, New York (2003), pp. 447–454.

J. Decker, A. Bers, A. K. Ram, and Y. Peysson, “Electron Cyclotron Current Drive by the Ohkawa Method in the Presence of Bootstrap Current,” *Proc. 30th European Physical Society (EPS) Conference on Controlled Fusion and Plasma Physics,* St. Petersburg, Russia, July 7–11, 2003. Online paper P3_205, September 2003, http://eps2003.ioffe.ru/PDFS/P3_205.PDF (January 14, 2004). CD-ROM, Europhysics Conference Abstracts (ECA) Vol. 27A, 2003 (eds. R. Koch and S. Lebedev; CD-ROM producers N. Vsesvetskii and N. Zhubr), Paper P3_205.

J. Decker, A. K. Ram, A. Bers, and Y. Peysson, “Current Drive by Electron Bernstein Waves in Spherical Tori,” *Bull. Am. Phys. Soc.* 48: 189 (2003).

P. C. Efthimion, G. Taylor, B. Jones, R. W. Harvey, A. K. Ram, A. P. Smirnov, T. Munsat, G. L. Bell, A. Bers, J. Decker, J. C. Hosea, R. Kaita, C. N. Lashmore-Davies, R. Majeski, D. A. Rasmussen, J. Spaleta, J. B. Wilgen, and J. R. Wilson, “Application of Electron Bernstein Wave Heating and Current Drive to High Beta Plasmas,” *Proc. 19th International Atomic Energy Agency (IAEA) Fusion Energy Conference,* Lyon, France, October 14–19, 2002. Online paper EX/P2-12, September 2003, http://www.iaea.org/programmes/ripc/physics/fec2002/pdf/exp2_12.pdf (November 15, 2003); Paper EX/P2-12, CD-ROM (Vienna, Austria), International Atomic Energy Agency, IAEA-CSP-19/CD, September 2003.

A. Parisot, S. J. Wukitch, A. Ram, R. Parker, Y. Lin, J. W. Hughes, B. LaBombard, P. Bonoli, and M. Porkolab, “Investigation of ICRF Coupling Resistance in Alcator C-Mod Tokamak,” *Proc. 15th Topical Conference on Radio Frequency Power in Plasmas,* Moran, Wyoming, May 19–21, 2003. A.I.P. Conf. Proc. 694 (ed. C. B. Forest), Melville, New York (2003), pp. 158–161.

Y. Peysson, J. Decker, A. Bers, and A. K. Ram, “Selfconsistent RF Driven and Bootstrap Currents,” *Proc. 19th International Atomic Energy Agency (IAEA) Fusion Energy Conference,* Lyon, France, October 14–

19, 2002. Online paper TH/P3-22, September 2003, http://www.iaea.org/programmes/ripc/physics/fec2002/pdf/thp3_22.pdf (November 15, 2003); Paper TH/P3-22, CD-ROM (Vienna, Austria), International Atomic Energy Agency, IAEA-CSP-19/CD, September 2003.

Y. Peysson, J. Decker, and R. W. Harvey, "Advanced 3-D Electron Fokker-Planck Transport Calculations," *Proc. 15th Topical Conference on Radio Frequency Power in Plasmas*, Moran, Wyoming, May 19–21, 2003. A.I.P. Conf. Proc. 694 (ed. C. B. Forest), Melville, New York (2003), pp. 495–498.

A. K. Ram, J. Decker, and A. Bers, "Relativistic Effects in Electron Bernstein Wave Current Drive," *Bull. Am. Phys. Soc.* 48: 216 (2003).

A. K. Ram, J. Decker, A. Bers, R. A. Cairns, and C. N. Lashmore-Davies, "Relativistic Effects in Heating and Current Drive by Electron Bernstein Waves," *Proc. 15th Topical Conference on Radio Frequency Power in Plasmas,* Moran, Wyoming, May 19–21, 2003. A.I.P. Conf. Proc. 694 (ed. C. B. Forest), Melville, New York (2003), pp. 392–395.

A. K. Ram, J. Decker, A. Bers, R. A. Cairns, and C. N. Lashmore-Davies, "Relativistic Effects in Heating and Current Drive by Electron Bernstein Waves," *Proc. 30th European Physical Society (EPS) Conference on Controlled Fusion and Plasma Physics,* St. Petersburg, Russia, July 7–11, 2003. Online paper P3_204, September 2003, http://eps2003.ioffe.ru/PDFS/P3_204.PDF (January 14, 2004). CD-ROM, Europhysics Conference Abstracts (ECA) Vol. 27A, 2003 (eds. R. Koch and S. Lebedev; CD-ROM producers N. Vsesvetskii and N. Zhubr), Paper P3_204.

A. K. Ram, B. C. Ross, D. J. Strozzi, and A. Bers, "Electrostatic Fields in Ionospheric Density Cavities and Their Effect on Ion Dynamics," *Eos (2003 American Geophysical Union Fall Meeting supplement)* 84(46), SM11C-1179 (2003).

A. K. Ram, D. J. Strozzi, B. C. Ross, and A. Bers, "Nonlinear Energization of Ionospheric Ions by Electrostatic Fields," *Proc. 7th International Workshop on the Interrelationship Between Plasma Experiments in Laboratory and Space (IPELS) Conference,* Whitefish, Montana, June 29–July 3, 2003, p. 16.

B. C. Ross, A. K. Ram, and A. Bers, "Resonant Modes and Ion Acceleration in Density-Depleted Plasma Cavities," *Bull. Am. Phys. Soc.* 48: 159 (2003).

A. Salcedo, R. J. Focia, A. K. Ram, and A. Bers, "Studies of Stimulated Raman Scattering in Laser Plasma Interactions," *Proc. 19th International Atomic Energy Agency (IAEA) Fusion Energy Conference,* Lyon, France, October 14–19, 2002. Online paper IF/P-01, September 2003, http://www.iaea.org/programmes/ripc/physics/fec2002/pdf/ifp_01.pdf (November 15, 2003); Paper IF/P-01, CD-ROM (Vienna, Austria), International Atomic Energy Agency, IAEA-CSP-19/CD, September 2003.

D. J. Strozzi, A. K. Ram, and A. Bers, "Coherent Ion Energization by Electrostatic Waves," *Proc. International Sherwood Fusion Theory Meeting,* Corpus Christi, Texas, April 28–30, 2003, Paper 2C27. Online paper 2C27, June 2003, http://www.sherwoodtheory.org/sherwood03/program/2C27.pdf (November 15, 2003).

D. J. Strozzi, A. K. Ram, A. Bers, and M. Shoucri, "Kinetic Simulation of Laser-Plasma Interactions," *Bull. Am. Phys. Soc.* 48: 45 (2003).

D. J. Strozzi, M. Shoucri, and A. Bers, "Study of Laser Plasma Interactions Using an Eulerian Vlasov Code," Proc. 18th International Conference on Numerical Simulation of Plasmas (ICNSP), Falmouth, Massachusetts, September 7–10, 2003, pp. 121–124. Online paper, November 2003, http://web.mit.edu/ned/ICNSP/ICNSP_BookofAbstracts.pdf, pp. 121–124 (December 15, 2003).

E. J. Synakowski, M. G. Bell, R. E. Bell, T. Bigelow, M. Bitter, W. Blanchard, J. Boedo, C. Bourdelle, C. Bush, D. S. Darrow, E. D. Fredrickson, D. A. Gates, M. Gilmore, L. R. Grisham, J. C. Hosea, D. W. Johnson, R. Kaita, S. M. Kaye, S. Kubota, H. W. Kugel, B. P. LeBlanc, K. Lee, R. Maingi, J. Manickam, R. Maqueda, E. Mazzucato, S. S. Medley, J. Menard, D. Mueller, B. A. Nelson, C. Neumeyer, M. Ono, F. Paoletti, H. K. Park, S. F. Paul, Y.-K. M. Peng, C. K. Phillips, S. Ramakrishnan, R. Raman, A. Rosenberg, P. M. Ryan, S. A. Sabbagh, C. H. Skinner, V. Soukhanovskii, T. Stevenson, D. Stutman, D. W. Swain, G. Taylor, A. Von Halle, J. Wilgen, M. Williams, J. R. Wilson, S. J. Zweben, X. Xu, R. Akers, R. E. Barry, P. Beiersdorfer, J. M. Bialek, B. Blagojevic, P. T. Bonoli, R. Budny, M. D. Carter, J. Chrzanowski, W. Davis, B. Deng, E. J. Doyle, L. Dudek, P. C. Efthimion, J. Egedal, R. Ellis, J. R. Ferron, M. Finkenthal, J. Foley, E. Fredd, A. Glasser, T. Gibney, R. J. Goldston, R. Harvey, R. E. Hatcher, R. J. Hawryluk, W. Heidbrink, K. W. Hill, W. Houlberg, T. R. Jarboe, S. C. Jardin, H. Ji, M. Kalish, J. Lawrance, L. L. Lao, K. C. Lee, F. M. Levinton, N. C. Luhmann, R. Majeski, R. Marsala, D. Mastravito, T. K. Mau, B. McCormack, M. M. Menon, O. Mitarai, M. Nagata, N. Nishino, M. Okabayashi, G. Oliaro, D. Pacella, R. Parsells, T. Peebles, B. Peneflor, D. Piglowski, R. Pinsker, G. D. Porter, A. K. Ram, M. Redi, M. Rensink, G. Rewoldt, J. Robinson, P. Roney, A. L. Roquemore, M. Schaffer, K. Shaing, S. Shiraiwa, P. Sichta, D. Stotler, B. C. Stratton, Y. Takase, X. Tang, R. Vero, W. R. Wampler, G. A. Wurden, X. Q. Xu, J. G. Yang, L. Zeng, and W. Zhu, “The National Spherical Torus Experiment (NSTX) Research Program and Progress Towards High Beta, Long Pulse Operating Scenarios,” *Proc. 19th International Atomic Energy Agency (IAEA) Fusion Energy Conference,* Lyon, France, October 14–19, 2002. Online paper OV2-2, September 2003, http://www.iaea.org/programmes/ripc/physics/fec2002/pdf/ov2_2.pdf (November 15, 2003); Paper OV2-2, CD-ROM (Vienna, Austria), International Atomic Energy Agency, IAEA-CSP-19/CD, September 2003.

G. Taylor, P. C. Efthimion, B. Jones, G. L. Bell, A. Bers, T. S. Bigelow, M. D. Carter, R. W. Harvey, A. K. Ram, D. A. Rasmussen, A. P. Smirnov, J. B. Wilgen, and J. R. Wilson, “Electron Bernstein Wave Research on NSTX and CDX-U,” *Proc. 15th Topical Conference on Radio Frequency Power in Plasmas,* Moran, Wyoming, May 19–21, 2003. A.I.P. Conf. Proc. 694 (ed. C. B. Forest), Melville, New York (2003), pp. 396–399.

G. Taylor, P. C. Efthimion, J. R. Wilson, G. L. Bell, T. S. Bigelow, M. D. Carter, D. A. Rasmussen, J. B. Wilgen, T. Peebles, S. Kubota, A. K. Ram, A. Bers, R. Temkin, R. W. Harvey, and A. P. Smirnov, “NSTX Electron Bernstein Wave (EBW) Research,” *Bull. Am. Phys. Soc.* 48: 173 (2003).

Reports

J. Decker, A. Bers, A. K. Ram, and Y. Peysson, “Electron Cyclotron Current Drive by the Ohkawa Method in the Presence of Bootstrap Current," Plasma Science and Fusion Center Report No. PSFC/JA-03-18 (Cambridge, Massachusetts: Massachusetts Institute of Technology, 2003).

A. K. Ram and A. Bers, “Excitation and Emission of Electron Cyclotron Waves in Spherical Tori," Plasma Science and Fusion Center Report No. PSFC/JA-03-15 (Cambridge, Massachusetts: Massachusetts Institute of Technology, 2003).

A. K. Ram, J. Decker, A. Bers, R. A. Cairns, and C. N. Lashmore-Davies, “Relativistic Effects in Heating and Current Drive by Electron Bernstein Waves,” Plasma Science and Fusion Center Report No. PSFC/JA-03-16 (Cambridge, Massachusetts: Massachusetts Institute of Technology, 2003).

D. J. Strozzi, A. K. Ram, and A. Bers, “Coherent Acceleration of Magnetized Ions by Electrostatic Waves With Arbitrary Wavenumbers," Plasma Science and Fusion Center Report No. PSFC/JA-03-14 (Cambridge, Massachusetts: Massachusetts Institute of Technology, 2003).

D. J. Strozzi, M. Shoucri, and A. Bers, “Study of Laser Plasma Interactions Using an Eulerian Vlasov Code,” Plasma Science and Fusion Center Report No. PSFC/JA-04-6 (Cambridge, Massachusetts: Massachusetts Institute of Technology, 2004).